eNeuro

Research Article: New Research | Cognition and Behavior

Mechanism of miR-132-3p Promoting Neuroinflammation and Dopaminergic Neurodegeneration in Parkinson's Disease

https://doi.org/10.1523/ENEURO.0393-21.2021

Cite as: eNeuro 2022; 10.1523/ENEURO.0393-21.2021

Received: 24 September 2021
Revised: 29 November 2021
Accepted: 2 December 2021

Mechanism of miR-132-3p promoting neuroinflammation and dopaminergic neurodegeneration in Parkinson's disease

Running title: *miR-132-3p*/GLRX in PD

Xin Gong, Mengyi Huang, Lei Chen*

Affiliation: Department of Neurosurgery, Hunan Provincial People's Hospital, The First Affiliated Hospital of Hunan Normal University, Changsha, Hunan 410005, P.R. China

***Corresponding Author:** Lei Chen, Department of Neurosurgery, Hunan Provincial People's Hospital, The First Affiliated Hospital of Hunan Normal University, No. 61, West Jiefang Road, Furong District, Changsha, Hunan 410005, P.R. China

E-mail: chenlei19821@163.com

Abstract

The major pathology in Parkinson's disease (PD) is neuron injury induced by degeneration of dopaminergic neurons and the activation of microglial cells. The objective of this study is to determine the effect and mechanism of miR-132-3p in regulating neuroinflammation and the degeneration of dopaminergic neuron in PD. The expressions of miR-132-3p in brain tissues of PD patients, LPS induced BV-2 cells and MPTP induced PD mouse models were detected. The effect of miR-132-3p and GLRX in cell viability, apoptosis and inflammation was verified in BV-2 cells. The activation of Iba1 in substantia nigra pars compacta and the loss of tyrosine hydroxylase were detected in PD mouse models and the mobility of mouse models was assessed as well. The targeting relationship between miR-132-3p and GLRX was confirmed by RIP and dual luciferase reporter gene assay. Elevated expression of miR-132-3p and decreased expression of GLRX were found in PD patients and cells models. Overexpression of miR-132-3p can induce activation of microglial cells, which can be reversed by GLRX overexpression. Collected evidence in both cell model and mouse models showed the effect of miR-132-3p in enhancing the activation of microglial cells and the loss of microglia cells, which was achieved by mediating GLRX.

Keywords: Parkinson's disease; *MiR-132-3p*; Neuroinflammation; Dopaminergic neuron; GLRX; MPTP

Significance statement

The purpose of this study is to explore the possible effect and mechanism of miR-132-3p/GLRX on neuroinflammation and the degeneration of dopaminergic neuron in Parkinson's disease (PD). This is important as no effective treatment is

available to cure PD and better understanding on how neuroinflammation and degeneration of dopaminergic neurons was regulated in PD will facilitate the proposal of therapeutic strategy. Future study should further validate the role and mechanism of miR-132-3p in regulating PD through GLRX before miR-132-3p can be proposed as a novel therapeutic target.

Introduction

Parkinson's disease (PD) is a neurodegenerative disease in elderly caused by degeneration of dopaminergic neurons mainly in the substantia nigra pars compacta (SNc), a region of the midbrain (Alizadeh, Kamrava, Bagher et al., 2019; Sveinbjornsdottir, 2016). Severe locomotor deficit, such as freezing of gait, is a typical phenomenon of PD, which refers to intermittent walking disturbance during walk initiation and turning (Strubberg & Madison, 2017). The etiology of PD is probably multifactorial and currently there is no available treatment that can attenuate the neurodegenerative process of the disease. Therefore, a clearer understanding of mechanizing driving PD progression would be beneficial for the proposal of therapeutic approach. A variety of molecular mechanisms that likely contribute to neuronal cell death have been described previously, including α-synuclein aggregation, mitochondrial dysfunction and noxious oxidant stress (Milanese, Gabriels, Barnhoorn et al., 2020). In addition, neuroinflammation is one of the hallmarks of PD and may induce the degeneration of midbrain dopamine neurons (Krashia, Cordella, Nobili et al., 2019). Therefore, therapeutic intervention would be a potential strategy to alleviate the progression of PD by interfering with neuroinflammation and degeneration of dopaminergic neurons.

MicroRNA (miRNA) is an endogenic RNA comprised of 21 to 24 nucleotides,

which controls gene transcription in combination with the 3' untranslated region of multiple targeted messenger RNAs (mRNAs) (Angelopoulou, Paudel, & Piperi, 2019; Li, Pan, Zhang et al., 2017). About ~1900 miRNAs that can be encoded by human genome (Strubberg & Madison, 2017). Among these miRNAs, *miR-132* has been frequently mentioned in many researches for its increased expression in neurons and for its implication in various neurodegenerative disorders. For example, the enhanced expression of *miR-132-3p* is related to chronic neuropathic pain (Leinders, Uceyler, Pritchard et al., 2016). *MiR-132*/Nurr1 axis was reported to have certain relationship with PD progression (Yang, Li, Li et al., 2019). Moreover, neuronal inflammation-induced epilepsy may be attenuated by *miR-132* by targeting TRAF6, along with inactivation of NF-κB and MEK/ERK pathways (Ji, Wang, Liu et al., 2018). *MiR-132* is positively associated with dopaminergic neuronal death (Qazi, Lu, Duru et al., 2021). Evidence in previous study pointed out that microglial cells medicated neuroinflammation triggered the cascade of inflammatory events leading to neuronal degeneration (Bassani, Vital, & Rauh, 2015; Hirsch & Hunot, 2009; Ye, He, Lu et al., 2018). However, it remains unclear how *miR-132-3p* is involved in neuroinflammation and dopaminergic neurodegeneration in PD.

GLRX is a small protein that catalyzes the glutathione-dependent disulfide oxidoreduction reactions in a coupled system (Wang, Liu, Liu et al., 2019). In models of PD, deficiency of GLRX aggravates neurodegeneration (Johnson, Yao, Siedlak et al., 2015). Meanwhile, previous study addressed that suppression of GLRX contributes to PD-relevant motor deficits and dopaminergic degeneration in mice (Verma, Ray, Bapat et al., 2020). Therefore, we speculated GLRX also has certain role to play in neuroinflammation and dopaminergic neurodegeneration in PD. Online software predicted that *miR-132-3p* was identified as an upstream regulatory factor of

GLRX. In this regards, this study aims to investigate the mechanism by which *miR-132-3p* regulates neuroinflammation and dopaminergic neuron degeneration in PD. Hence, exploring the interactions between *miR-132-3p*/GLRX, dopaminergic neurodegeneration and neuroinflammation may be of great importance for the proposal of a latent therapeutic alternative for PD.

The main aims of the present study were to determine (1) whether *miR-132-3p* expression level is significantly altered in patients with PD as compared with healthy controls; (2) whether *miR-132-3p* is responsible for microglial activation and neuronal injury; (3) whether *miR-132-3p* affects the dopaminergic neuron degeneration and neuroinflammation in PD mouse models; and (4) whether *miR-132-3p* intensifies PD by inhibiting GLRX.

Materials and methods

Collection of clinical brain tissues

The study was carried out according to the *Declaration of Helsinki*. The study protocol concerning human was approved by the Ethics Committee of Hunan Provincial People's Hospital (No.: 202004), and written informed consent from family members of included subjects was obtained. This study was not pre-registered and no sample calculation was performed. After death, the midbrain tissues were obtained from 5 patients with PD (3 males and 2 females, 55.8 ± 7.09 years old) and 5 healthy controls (3 males and 2 female, 59.8 ± 8.07 years old) matched for age. The brain tissues were collected and stored in liquid nitrogen, in which the total RNA and total protein were stored at -80°C refrigerator. The diagnosis of PD was performed by at least two or more experienced neurologists based on the clinical diagnostic criteria proposed by International Parkinson and Movement Disorder Society (Postuma,

Poewe, Litvan et al., 2018). The included PD patients were excluded from secondary PD, tumor or metabolic disturbance. The healthy controls were excluded from disorders related to nervous system.

Cell culture

The BV-2 microglial cells, human neuroblastoma cell line SH-SY5Y and human embryonic kidney (HEK) 293T cells were supplied by American Type Culture Collection (ATCC, Manassas, Virginia, USA). The BV-2 and HEK293T cells were soaked in Dulbecco's modified Eagle medium (DMEM, Gibco, Grand Island, NY, USA), and SH-SY5Y cells were immersed in DMEM/Nutrient Mixture F-12 (DMEM/F12, Gibco). The culture medium contained 10% fetal bovine serum (FBS), 100U/mL penicillin and 100 mg/mL streptomycin. Cell culture was kept at 37ºC in a humidified atmosphere containing 5% CO_2. The inflammation of BV-2 cells was induced by 0.1 μg/mL lipopolysaccharide (LPS) for 24 h. The cell passage of cell lines shall not exceed 10 times.

Cell transfection

The *miR-132-3p* mimic (miRNA mimic refers to a sequence that can simulate specific endogenous miRNA), mimic NC, *miR-132-3p* inhibitor (miRNA inhibitor refers to a sequence that can interfere with miRNA), inhibitor NC, overexpressing GLRX (GLRX) and pcDNA3.1 were synthesized and purchased from GenePharma (Shanghai, China). Cell transfection was conducted by using the Lipofectamine 3000 reagent (Invitrogen, Carlsbad, CA, USA). The transfection dose of overexpression plasmids was 2 μg and the dose of mimic and inhibitor was 50 nM. Cells were treated by LPS for 24 h before following experiments were conducted.

qRT-PCR

TRIzol (Invitrogen) was employed to extract the total RNA of tissues or cells,

and the reverse transcription was conducted by using the reverse transcription kit (TaKaRa, Tokyo, Japan). The expression of gene was quantitated by LightCycler 480 fluorescence quantitative PCR instrument (Roche, Indianapolis, IN, USA), and reaction condition was instructed by the fluorescence quantitative PCR kit (SYBR Green Mix, Roche Diagnostics, Indianapolis, IN). The thermal cycle parameters were 95℃ for 10 s, followed by 45 cycles of 95℃ for 5 s, 60℃ for 10 s and 72℃ for 10 s. A final extension was carried out at 72°C for 5 min. The quantification of mRNA was normalized to β-actin and miRNA to U6. The fold changes were calculated by the $2^{-\Delta\Delta Ct}$ method. The formula is as follows: $\Delta\Delta Ct = [Ct_{(target\ gene)}\text{-}Ct_{(reference\ gene)}]_{experimental\ group}\text{-}[Ct_{(target\ gene)}\text{-}Ct_{(reference\ gene)}]_{control\ group}$. All primers are shown in **Table 1**.

Western blot

For collection of protein samples, RIPA lysis buffer (Beyotime Biotech, Shanghai, China) was utilized to treat cells or tissues. Following determination of protein concentration with a BCA kit, the proteins in the corresponding volume were mixed with loading buffer (Beyotime) and subjected to denaturation in a boiling-water bath for 3 min. Electrophoresis was embarked at 80 V for 30 min, and then for 1 ~ 2 h at 120 V when bromphenol blue reached the separation gel. The proteins were transferred onto membranes at 300 mA for 60 min in an ice bath. Then, the membranes were rinsed 1 ~ 2 min with washing solution and inactivated in the blocking solution at room temperature for 60 min, or sealed overnight at 4℃. Following incubation with the primary antibodies against β-actin (ab8226, 1 μg/mL) and GLRX (ab45953, 1:250) (Abcam, Cambridge, MA, USA) at room temperature in a shaking table for 1 h, the membranes were washed with the washing solution for 3 × 10 min and incubated with the secondary antibody for 1 h at room temperature. The membranes were washed thrice for 10 min and exposed to developing liquid for color

development. Then, the membranes were observed in chemiluminecence imaging analysis system (Gel Doc XR, Bio-Rad).

ELISA

The ELISA kit (R&D Systems, Minneapolis, MN, USA) was adopted to determine the contents of TNF-α, IL-6 and IL-1β in the cell supernatant. All operations were performed in accordance with the instructions of the ELISA kit.

Co-culture of BV-2 and SH-SY5Y cells

The effect of microglial activation on SH-SY5Y cells was studied by co-culture of BV-2 cell supernatant and SH-SY5Y cells. The supernatant of BV-2 cells in each group was collected and filtered with a 0.45 μm filter. SH-SY5Y cells were seeded onto the six-well plates for cell culture till the density of SH-SY5Y cells reached 70%. The supernatant of BV-2 cells and DMEM/F12 containing 10% FBS were mixed at a ratio of 1:1, and the mixture was co-cultured with SH-SY5Y cells for 24 h.

CCK-8 assay

The SH-SY5Y cells were seeded onto 96-well plates, and cells in each well received 100 μL pre-diluted cell suspension (1×10^5 cells/mL). Twenty-four h later, SH-SY5Y cells were grown in conditioned medium of BV-2 cells for 24 h. The experiment was designed with three replicates. Ten microliters of CCK-8 solution (Dojindo, Tokyo, Japan) was added to each well for 2 h of incubation. The optical density (OD) at 450 nm wavelength was assessed.

Flow cytometry

After SH-SY5Y cells (10^5 cells/mL) were incubated with conditioned medium of BV-2 cells for 24 h, 3 mL cell suspension from each sample was transferred into a 10 mL centrifuge tube for 5 min of centrifugation at 500 rpm. After removal of culture

medium, cells were washed with phosphate-buffered saline (PBS) and centrifuged at 500 rpm for 5 min. The supernatant was discarded. Then, cells were resuspended in 100 μL of binding buffer, and then gently mixed with 5 μL Annexin V-FITC and 5 μL PI for incubation for 15 min in the dark. The fluorescence of FITC and PI was examined by flow cytometry, and the apoptosis rate was analyzed.

RNA immunoprecipitation (RIP)

Following wash twice with precooled PBS, cells were centrifuged at 1,500 rpm for 5 min and lysed with equivoluminal RIP lysis buffer. The magnetic beads were resuspended in 100 μL RIP Wash Buffer followed by 30 min of incubation with 5 μg antibody against Ago2 (ab186733, 1:30, Abcam) or IgG (ab172730, negative control) at room temperature. Cells in the centrifuge tube were placed on a magnetic separation rack to discard the supernatant. Following incubation with 500 μL RIP Wash Buffer for vortex oscillation twice, cells were given 500 μL of RIP Wash Buffer for vortex oscillation and placed on ice. The magnetic bead tube was transferred to the magnetic separation rack, and the supernatant was removed. After that, cells in each tube received 900 μL of RIP Immunoprecipitation Buffer. Cell lysates were centrifuged at 14,000 rpm at 4℃ for 10 min, and 100 μL of supernatant was pipetted into the magnetic bead-antibody complex for incubation overnight at 4℃. The complex processed centrifugation with supernatant removed. Then, the centrifuge tube received 500 μL of RIP Wash Buffer for vortex oscillation and cell supernatant was abandoned before the sediments were washed for six times. The magnetic bead-antibody complex was resuspended in 150 μL of Proteinase K Buffer and incubated at 55℃ for 30 min. Then, the samples were put in the magnetic separation rack to remove the supernatant. The gene expression was analyzed by qRT-PCR after RNA extraction.

Dual-luciferase reporter assay

The binding site of *miR-132-3p* and GLRX was predicted by the online prediction software StarBase (http://starbase.sysu.edu.cn/). The mutated type and wild type sequences in the binding sites were designed and cloned into pGL3-Promoter luciferase plasmid (Promega, Madison, WI, USA), namely mut-GLRX and wt-GLRX. Then, mut-GLRX or wt-GLRX was cotransfected with *miR-132-3p* mimic or *miR-132-3p* inhibitor, respectively, into HEK-239T cells or pRL-TK (Promega). After that, Renilla luciferase activity and Firefly luciferase activity were determined by dual-luciferase reporter gene assay kit (Promega). Renilla luciferase activity was deemed as the internal control, and the ratio between the activities of Firefly luciferase and Renilla luciferase was calculated as the relative activity.

PD mouse model

Six-month-old male C57BL/6J mice (n = 24) were purchased from the Shanghai SLAC Laboratory Animal Co., Ltd (Shanghai, China). All animal handling and experimental procedures were approved by the Animal Care and Use Committee of Hunan Provincial People's Hospital (No.: 202004). Mice were allowed food and water ad libitum and housed in rooms maintained at 24 ± 1°C and 60 ~ 80% humidity using a 12-hour dark cycle. The following experiments were conducted after one week of feeding. The study consisted of four groups of six mice each (random grouping by an Excel random number generator): the MPTP, Saline, *miR-132-3p* antagomir and antagomir NC groups. Mice in the MPTP group were intraperitoneally injected with 30 mg/kg MPTP (1-methyl-4-phenyl-1,2,3,6-tetrahydropyridine, Sigma-Aldrich, St. Louis, Missouri, USA) every day for 5 consecutive days (Hu, Zhang, Wang et al., 2019), and the mice of the Saline group were intraperitoneally injected with the same amount of Saline every day for 5 consecutive days. Mice in the MPTP+*miR-132-3p*

antagomir group or MPTP+antagomir NC group were injected with MPTP the next day after stereotactic injection of *miR-132-3p* antagomir or antagomir NC (20 nM, total volume of 5 μL, GenePharma, Shanghai, China) into targeted brain areas of mice.

Stereotactic injection

After anesthesia of mice with ketamine (100 mg/kg) and xylazine (10 mg/kg) by intraperitoneal injection, the head of mouse was fixed to expose the skull. The intracerebral injection was performed on the following coordinates: -2.8 mm anteroposterior, -1.2 mm mediolateral, and -4.3 mm dorsoventral. Five microliters of *miR-132-3p* antagomir suspension or antagomir NC suspension was injected into SNc by using a 10 μL stereotactic catheter (1 μL/5 min). The needle remained in place for 5 min after complete injection then slowly removed. The mice were placed on a pad until recovery from the anesthesia. The healthy conditions of mice were monitored on the following 5 days, during which mice were subjected to acesodyne and local disinfection. The activity of mice after injection was recorded. No mouse was died during the whole experiments.

Behavioral tests

One week after establishment of PD mouse models, the behavioral tests were commenced. Motor coordination ability of experimental animals was investigated with the rotarod test. Before the experiments, animals were placed on rotating lanes for 5 min. Then, mice were trained for 2 min at a fixed speed of 4 rpm. After training, the rotational speed was accelerated uniformly from 4 rpm to 40 rpm within 60 s. The time of mice falling off the rotating rod was recorded. The open field test was carried out to evaluate the autonomous and exploratory behaviors of experimental animals in novel environments. Mice were individually placed into the center of an open field

box (38 × 38 cm) in a noise and light-controlled room. The spontaneous locomotor activities (central-area distance and whole-area distance) of each mouse were recorded and analyzed. The relative time of mouse falling from the rotating rod and the relative distance of mouse staying in the open field were recorded. Relative time and relative distance is the ratio of time or distance of experimental mouse/control mouse.

Brain tissue collection

About 24 h after behavior test, ketamine (100 mg/kg) and xylaafine (10 mg/kg) were given to mouse for anesthesia through intraperitoneal injection. The heart was exposed and mouse (n = 6) in each group was perfused with 200 ml normal saline through ventriculus sinister. The skull was opened and the brain tissues were collected and isolated. Part of the brain tissues was stored at -80°C refrigerator for qRT-PCR and the rest brain tissues were fixed in 4% triformol for 48 h for fluorescence in situ hybridization (FISH), immunofluorescence and immunohistochemistry.

Fluorescence in situ hybridization (FISH)

The 4 μm paraffin sections were de-paraffinized with xylene and gradient alcohol (xylene soak for 10 min, refresh xylene for another 10 min, 50% xylene soaking for 10 min, absolute ethanol for 5 min, refresh absolute ethanol for another 5 min, 95% ethanol for 5 min, 90% ethanol for 5 min, 80% ethanol for 5 min and 70% ethanol for 5 min) before PBS wash. Sections were digested with 37℃ protease K for 15 min, washed with PBS for 2 × 5 min, pre-hybridized at 55℃ constant temperature, and incubated with digoxigenin-labeled (Exiqon, Vedbeak, Denmark) *miR-132-3p* probes overnight at incubator with 55℃ constant temperature. Then, sections were subsequently washed with 5 × SSC buffer, 1 × SSC, and 0.2 × SSC buffer for 2 × 5 min at 55℃, followed by 5 min of wash with 0.2 × SSC buffer at room temperature, 10 min of inactivation

with 0.3% hydrogen peroxide-methanol solution, and 3 × 5 min of PBS wash. After that, sections underwent three times of incubation each for 1 h: first blocked with normal serum blocking buffer at room temperature, second probed with mouse anti-DIG at room temperature, and then incubated with polymer anti-mouse. After each incubation, sections were washed three times with PBS for 5 min. Sections were stained with DAB for 5 ~ 10 min and washed with tap water for 10 min, prior to 2 min of hematoxylin counterstaining, hydrochloric ethanol differentiation and 10 min of tap water wash. These sections were sealed with neutral balata for observation under a microscope after dehydration and permeabilization. The ratio of positive cell numbers to total number of cells was calculated. DAPI was used for staining of cell nucleus and Iba1 was used to labelled microglial cells.

Immunofluorescence

Sections were incubated for 60 min at 60℃, dewaxed with xylene and washed with distilled water. Following antigen retrieval with 0.01 mol/l sodium citrate, sections were subjected to 10 min of incubation with 3% H_2O_2. Then, sections were washed with PBS for 3 × 5 min, and inactivated with 5% normal goat serum for 30 min at room temperature. Sections were cultured with the primary antibody against tyrosine hydroxylase (ab137869, 1:200, Abcam), Iba1 (ab178846, 1:500, Abcam) or GLRX (ab45953, 1 μg/ml, Abcam) overnight at 4℃, while sections in negative control group contains corresponding antigens and were incubated with PBS. After that, sections were washed three times with PBS and incubated with FITC-labeled secondary antibody (ab6785, 1:1000, Abcam) at room temperature for 1 h. Then, the secondary antibody was removed, and cells were subjected to 5 min of staining with DAPI and 3 × 5 min of PBS wash. Before pictures were captured by fluorescence microscope, sections were given glycerophosphoric acid for sealing.

StereoInvestigator (MBF Bioscience) was used for stereological analysis on the total number of TH positive neurons and Iba1 positive cells for every sixth coronal section through the midbrain. After the the SN pars compacta with a × 4 objective was delineated, cells were counted under × 60 magnification using ImageJ and following parameters: 8 μm height of an optical disector, 50 × 50 μm counting frame, 100 × 100μm area of a grid. The error coefficient of less than 0.10 was acceptable. All sections were quantified in a blinded manner.

Immunohistochemistry

Following 60 min of bake, sections were dewaxed by xylene and washed with distilled water. Before 30 min of inactivation with normal goat serum at room temperature, sections underwent the following steps: antigen retrieval with 0.01 mol/L sodium citrate, 10 min of reaction with 3% H_2O_2 and three times of PBS wash for 5 min. The sections were inactivated with 5% normal goat serum for 30 min at room temperature. After that, sections were incubated with antibody against GLRX (ab45953, 1 μg/mL, Abcam) overnight at 4°C, while sections in negative control group contains corresponding antigens and were incubated with PBS. Sections were then subjected to three times of PBS wash and 1 h of incubation with secondary antibody (ab6785, 1:1000, Abcam). DAB was used for color development, and sections were given three times of PBS wash to terminate the color reaction (1 ~ 3 min). The nucleus was stained with hematoxylin for 3 min, and sections were dehydrated, permeabilized and sealed. The percentage of positive cells was counted. Images were analyzed using Image J software (version 1.46, National Institutes of Health).

Statistical analysis

Experiments and statistical analysis were performed by different personnel.

Statistical analysis was conducted utilizing GraphPad Prism 7 software, and data are displayed as the mean ± standard deviation (SD). The normal distribution of data was detected by Kolmogorov-Smirnov test, D'Agostino, Pearson omnibus normality test or Shapiro-Wilk normality test. All data were complied with normal distribution. The *T*-test was employed for comparisons between two groups. The one-way analysis of variance was adopted followed by Tukey's multiple comparison tests for comparisons among multiple groups. *P* values of significance were those less than 0.05.

Results

Highly expressed *miR-132-3p* and lowly expressed GLRX in midbrain tissues of patients with PD

The expressions of *miR-132-3p* and GLRX in midbrain tissues of patients with PD and in healthy controls were determined by qRT-PCR and Western blot. The results of qRT-PCR manifested compared with control group, *miR-132-3p* in midbrain tissues of patients with PD was increased by 1.45 ± 0.33 fold (**Fig. 1A**, $P < 0.05$). Furthermore, analyses of qRT-PCR and Western blot exhibited that the mRNA and protein expressions of GLRX in the tissues of patients with PD were decreased to respectively 0.63 ± 0.15 fold and 0.69 ± 0.18 fold (**Fig. 1B-C**, $P < 0.05$, vs the Control group). These finding indicated that *miR-132-3p* and GLRX may be implicated in the progression of PD.

Knockdown of *miR-132-3p* inhibits LPS-induced inflammatory response in BV-2 cells

The BV-2 cells were transfected with *miR-132-3p* inhibitor or inhibitor NC prior to 0.1 μg/mL LPS or PBS treatment to explore the effect of *miR-132-3p* on LPS-induced inflammatory response in BV-2 cells. Results of qRT-PCR presented

that LPS treatment elevated *miR-132-3p* expression in BV-2 cells by 1.74 ± 0.21 fold ($P < 0.01$, vs the PBS group), while transfection with *miR-132-3p* inhibitor suppressed the mRNA level of *miR-132-3p* (**Fig. 2A**, $P < 0.001$, LPS + miR-132-3p inhibitor vs the LPS+inhibitor NC group: 0.45 ± 0.06 fold vs 1.68 ± 0.19 fold). Additionally, the enhanced expressions of inflammatory cytokines IL-6 (2.98 ± 0.32 fold), TNF-α (4.34 ± 0.46 fold) and IL-1β (3.73 ± 0.37 fold) in BV-2 cells were occurred in response to LPS induction ($P < 0.001$, vs the PBS group), whereas these levels were somewhat attenuated in cells transfected with *miR-132-3p* inhibitor (**Fig. 2B**, $P < 0.01$, LPS+miR-132-3p inhibitor vs the LPS+inhibitor NC group: TNF-α: 2.38 ± 0.26 fold vs 4.18 ± 0.45 fold; IL-1β: 1.69 ± 0.18 fold vs 3.68±0.41 fold; IL-6: 1.84 ± 0.21 fold vs 3.22 ± 0.29 fold). The contents of inflammatory cytokines in the supernatant of BV-2 cells were determined by ELISA, and the results showed that the rises in contents of IL-1β (453.29 ± 66.47 vs 16.74 ± 2.58 pg/ml), IL-6 (386.47 ± 45.79 vs 13.27 ± 2.18 pg/ml) and TNF-α (734.48 ± 114.37 vs 84.56 ± 18.24 pg/ml) in the LPS group ($P < 0.001$, vs the PBS group). Compared with LPS+inhibitor NC group, contents of IL-1β (198.37±23.51 vs 537.28±68.34 pg/ml), IL-6 (167.28±24.35 vs 415.27±48.61 pg/ml) and TNF-α (346.57±72.44 vs 672.35±94.27 pg/ml) in the LPS+*miR-132-3p* inhibitor group were suppressed (**Fig. 2C**, $P < 0.01$). The above findings suggested that suppression on *miR-132-3p* may repress LPS-induced inflammatory response in BV-2 microglial cells.

miR-132-3p overexpression enhances inflammatory response in BV-2 cells

Based on the previous experimental results, downregulation of *miR-132-3p* can inhibit LPS-induced activation and inflammation of microglial cells. However, whether upregulation of *miR-132-3p* can induce microglial activation and inflammation is still unknown. Toward this end, BV-2 cells were transfected with

miR-132-3p mimic or mimic NC. We found that overexpression of *miR-132-3p* in miR-132-3p mimic group had increased the mRNA levels of *miR-132-3p* by 6.84 ± 0.53 fold (**Fig. 3A,** $P < 0.01$). Additionally, miR-132-3p mimic group had elevated mRNA expressions of TNF-α (1.89 ± 0.19 fold vs 0.92 ± 0.12 fold), IL-1β (2.15 ± 0.22 fold vs 1.06 ± 0.15 fold), IL-6 (1.75 ± 0.16 fold vs 1.13 ± 0.11 fold) when compared with mimic NC group (**Fig. 3B,** $P < 0.01$). ELISA showed that TNF-α (247.63 ± 29.14 vs 82.78 ± 15.69 pg/ml), IL-1β (172.59 ± 19.37 vs 15.94 ± 1.83 pg/ml), IL-6 (134.76 ± 16.72 vs 15.36 ± 1.87 pg/ml) in the supernatant of BV-2 cells was also elevated in miR-132-3p mimic group in contrast to mimic NC group (**Fig. 3C**, $P < 0.01$). The results demonstrated that overexpression of *miR-132-3p* may induce the activation and inflammatory response of microglial cells.

Activated microglial cells by *miR-132-3p* cause neuronal injury

To investigate the role of microglial activation in neuronal injury, SH-SY5Y cells were cultured in conditioned medium of BV-2 cells that were transfected with inhibitor NC or *miR-132-3p* inhibitor and stimulated with LPS. The findings of CCK-8 assay addressed that the viability of SH-SY5Y cells in the LPS group was decreased to 43.86 ± 3.86% compared with PBS group ($P < 0.001$), while LPS+*miR-132-3p* inhibitor group possessed higher cell viability than that in the LPS+inhibitor NC group (**Fig. 4A**, $P < 0.01$, 71.61 ± 6.23% vs 50.27 ± 4.14%). Flow cytometry assessed that LPS stimulation heightened the apoptotic rate of SH-SY5Y cells (**Fig. 4B**, $P < 0.001$, 37.84 ± 2.73% vs 8.67 ± 1.23%), but treatment with *miR-132-3p* inhibitor lowered cell apoptotic rate (**Fig. 4B**, $P < 0.001$, 19.34 ± 2.27% vs 40.25 ± 3.16%,).

Meanwhile, the effect of *miR-132-3p* overexpression on neuronal injury was explored. Accordingly, SH-SY5Y cells were cultured in conditioned medium, in

412 which BV-2 cells were transfected with mimic NC or *miR-132-3p* mimic. We
413 discovered that upregulation of *miR-132-3p* reinforced cell apoptotic rate (16.83 ±
414 2.37% vs 8.25 1.43%) and diminished the viability of SH-SY5Y cells (71.35 ± 9.61%
415 vs 93.15 ± 8.63%) (**Fig. 4C-D**, $P < 0.05$). Collectively, the activated microglial cells
416 by *miR-132-3p* may lead to neuronal injury.

417 ***MiR-132-3p* is an upstream regulatory factor of GLRX**

418 After knockdown or overexpression of *miR-132-3p* in BV-2 cells, the mRNA and
419 protein expressions of GLRX were evaluated by qRT-PCR and Western blot. We
420 found that enhanced GLRX expression in miR-132-3p inhibitor group when
421 compared with inhibitor NC group (**Fig. 5A-B**, $P < 0.05$, mRNA: 1.76 ± 0.21 fold vs
422 1.09±0.12 fold; protein: 1.58 ± 0.23 fold vs 0.95 ± 0.13 fold), while miR-132-3p
423 mimic group had repressed level of GLRX compared with mimic NC group (**Fig.**
424 **5A-B**, $P < 0.05$, mRNA: 0.54 ± 0.07 fold vs 0.94 ± 0.11 fold; protein: 0.64 ± 0.11 fold
425 vs 0.96 ± 0.16 fold). Subsequently, the RIP experiment was applied to verify the
426 relationship of *miR-132-3p* to GLRX mRNA, and the results manifested that
427 compared with IgG antibody group, substantial GLRX mRNA can be recruited in
428 Ago2 complex (2.15 ± 0.24 fold vs 0.12 ± 0.03 fold, **Fig. 5C**, $P < 0.001$). After LPS
429 treatment, elevated expression of *miR-132-3p* was found and increased GLRX mRNA
430 was recruited in Ago2 complex (2.45 ± 0.36 fold vs 1.68 ± 0.23 fold, **Fig. 5D**, $P <$
431 0.05). Considering the directing binding of miR-132-3p with GLRX mRNAcannot be
432 proved by RIP as the regulation of other miRNAs or target genes cannot be excluded,
433 we then applied dual luciferase reporter gene assay to verify the binding. The binding
434 site of *miR-132-3p* to the 3'-UTR on GLRX mRNA was predicted by StarBase (**Fig.**
435 **5E**). The above result was verified by dual-luciferase reporter assay, which displayed
436 that HEK293T cells cotransfected with wt-GLRX and *miR-132-3p* mimic had

decreased luciferase activity by 62.33 ± 8.17% than cells cotransfected with wt-GLRX and mimic NC ($P < 0.01$). However, the relative luciferase activity in cells cotransfected with mut-GLRX and *miR-132-3p* mimic was not statistically different from cells cotransfected with mut-GLRX and mimic NC (**Fig. 5F**, $P > 0.05$, 108.67 ± 13.52% vs 93.16 ± 11.47%). The above results indicated that *miR-132-3p* may target GLRX and negatively regulate expression of GLRX.

GLRX mitigates neuronal injury and inhibits activation of microglial cells induced by *miR-132-3p*

To explore whether *miR-132-3p* promotes microglial inflammation and neuronal injury through mediating GLRX, BV-2 cells were transfected *miR-132-3p* mimic or cotransfected *miR-132-3p* mimic and plasmid overexpressing GLRX. Results of qRT-PCR and Western blot highlighted that transfection with *miR-132-3p* mimic lead to suppressed mRNA and protein expression levels of GLRX by 0.58 ± 0.08 fold and 0.64 ± 0.11 fold, whereas the coeffect of *miR-132-3p* mimic and plasmid overexpressing GLRX increased the expression of GLRX compared with transfection with *miR-132-3p* mimic alone (**Fig. 6A-B**, $P < 0.05$, mRNA: 2.46 ± 0.31 fold vs 0.58 ± 0.08 fold; protein: 1.85 ± 0.28 fold vs 0.64 ± 0.11 fold). Furthermore, the detections on mRNA expressions and contents of inflammatory cytokines revealed that cells in the *miR-132-3p* mimic+GLRX group had lower mRNA expression levels and contents of TNF-α (1.23 ± 0.14 fold vs 2.16 ± 0.22 fold), IL-6 (0.87 ± 0.11 fold vs 1.68 ± 0.18) and IL-1β (1.26 ± 0.12 fold vs 1.94 ± 0.18 fold) than in the *miR-132-3p* mimic group (**Fig. 6C**, $P < 0.01$). ELISA detection showed that the contents of TNF-α (115.86 ± 12.43 vs 218.37 ± 26.49 pg/ml), IL-1β (49.37 ± 6.68 vs 159.38 ± 18.32 pg/ml), IL-6 (31.27 ± 5.39 vs 124.38 ± 21.15 pg/ml) in the supernatant of BV-2 cells were suppressed in miR-132-3p mimic+GLRX group when compared with

462 miR-132-3p mimic group (**Fig. 6D**, $P < 0.01$). Then, SH-SY5Y cells were grown in
463 the conditioned medium of BV-2 cells. The findings of CCK-8 assay and flow
464 cytometry described the increase in cell viability (97.39 ± 7.65% vs 73.62 ± 8.51%,
465 **Fig. 6E**, $P < 0.05$) and the decrease in cell apoptotic rate (9.66 ± 2.16% vs 17.59 ±
466 2.67%, **Fig. 6F**, $P < 0.01$) in the *miR-132-3p* mimic+GLRX group compared with the
467 *miR-132-3p* mimic group. These data suggested that overexpression of GLRX may
468 reverse the effect of *miR-132-3p* upregulation on microglial activation and neuronal
469 injury.

470 **Suppression of *miR-132-3p* alleviates MPTP-induced neuroinflammation and**
471 **dopaminergic neurodegeneration in PD mouse models**

472 Mice were subjected to stereotactic injection of *miR-132-3p* antagomir and given
473 MPTP by intraperitoneal injection to probe the role of *miR-132-3p* in
474 neuroinflammation and dopaminergic neuron degeneration of MPTP-induced PD
475 mouse. The results of FISH presented that injection with MPTP elevated *miR-132-3p*
476 expression in SNc of mice by 196.37 ± 17.39% ($P < 0.001$), while the following
477 exposure to MPTP+*miR-132-3p* antagomir repressed the level of *miR-132-3p* (**Fig.**
478 **7A**, $P < 0.01$, 125.59 ± 12.67% vs 179.34 ± 14.34%). Immunohistochemistry results
479 displayed that there were enhanced expression of GLRX in the MPTP+*miR-132-3p*
480 antagomir group ($P < 0.001$, vs the MPTP+antagomir NC group, 87.25 ± 12.57% vs
481 57.16 ± 6.28%) and decreased level of GLRX in the MPTP group by 53.47 ± 6.39%
482 (**Fig. 7B**, $P < 0.01$, vs the Saline group). FISH and immunofluorescence were applied
483 to detect the expressions of miR-132-3p and GLRX in microglial cells. The results
484 showed that miR-132-3p expression of SNc of mice in MPTP group was increased by
485 2.16 ± 0.36 fold, while GLRX expression was suppressed by 0.46 ± 0.11 fold when
486 compared with Saline group. Comparisons between MPTP+miR-132-3p antagomir

group and MPTP+antagomir NC group demonstrated that miR-132-3p expression was suppressed (miR-132-3p: 1.58 ± 0.27 fold vs 2.34 ± 0.38 fold) and GLRX expression was elevated (GLRX: 0.84 ± 0.18 fold vs 0.53 ± 0.10 fold) in miR-132-3p antagomir group (**Fig. 7C-D**, $P < 0.01$). Co-location analysis showed miR-132-3p expression in microglial cells accounted for 40% of miR-132-3p expression in tissues, while the expression of GLRX in microglial cells accounted for 55% of GLRX expression in tissues (**Fig. 7C-D**). Additionally, immunofluorescence of Iba1 exhibited that the microglial activation was increased in MPTP group (619.74 ± 88.90 vs 174.83 ± 23.03 cells/mm^2, $P < 0.001$) and decreased in MPTP+*miR-132-3p* antagomir group (417.36 ± 74.78 vs 595.72 ± 78.02 cells/mm^2, **Fig. 7E**, $P < 0.01$). Analysis of qRT-PCR showed that MPTP treatment potentiated the mRNA levels of inflammatory cytokines TNF-α (1.68 ± 0.29 fold), IL-1β (1.79 ± 0.28 fold), IL-6 (1.84 ± 0.32 fold) in brain tissues of mice ($P < 0.01$), whereas MPTP+*miR-132-3p* antagomir diminished the expressions of TNF-α (1.26 ± 0.21 fold vs 1.76 ± 0.30 fold), IL-1β (1.22 ± 0.19 fold vs 1.72 ± 0.31 fold), IL-6 (1.34 ± 0.23 fold vs 1.81±0.28 fold) (**Fig. 7F**, $P < 0.05$). Then, the assessment of the dopaminergic neuron loss by immunofluorescence of tyrosine hydroxylase illustrated that tyrosine hydroxylase-positive neurons in SNc of mice were significantly decreased in the MPTP group ($P < 0.001$, 155.83 ± 25.97 vs 621.37 ± 91.97 cells/mm^2) and markedly increased in the MPTP+*miR-132-3p* antagomir group (401.72 ± 58.83 vs 177.83 ± 32.00 cells/mm^2, **Fig. 7G**, $P < 0.01$). The rotarod test and open field test were utilized to observe the motor ability of mice. In the rotarod test, mice in the MPTP group showed poor balance and coordination by suppressing the time to 57.38±12.37%, while mice in the MPTP+*miR-132-3p* antagomir group exhibited better balance and coordination (84.72 ± 15.46 vs 52.43 ± 9.27%) (**Fig. 7H**, $P < 0.01$). In the open field test, MPTP injection suppressed the

spontaneous locomotor activities (whole area: 53.27 ± 8.91%, central area: 42.35 ± 6.28%), whereas MPTP+*miR-132-3p* antagomir increased the spontaneous locomotor activities (whole area: 82.47 ± 13.67 vs 48.37 ± 7.21%; central area: 78.61 ± 11.59 vs 46.52 ± 7.38%) (**Fig. 7H**, $P < 0.01$). The above results indicated that MPTP injection may induce dopaminergic neurodegeneration and neuroinflammation of mice, while depletion of *miR-132-3p* may ameliorate the dopaminergic neuron degeneration and neuroinflammation of PD mouse.

Discussion

Neuroinflammation is a characteristic of neurodegenerative diseases, including PD, in which microglia confer pathogenic and exacerbating effects (J, 2020; Lull & Block, 2010). Furthermore, the notable hallmark of PD is the degeneration of dopaminergic neurons in the SNc (Mead, Kim, Miller et al., 2017). Herein, BV-2 cells and SH-SY5Y were utilized in current study to explore the effect of *miR-132-3p* on inflammation of microglial cells and neuronal injury. We have reported that *miR-132-3p* is abnormally upregulated, a change positively connected with the inflammatory response of microglial cells. We demonstrated that the activated microglial cells caused by *miR-132-3p* leads to increased cell apoptotic rate and diminished viability of neuroblastoma cells. However, *miR-132-3p* was also reported to alleviate neuron apoptosis and impairments of learning and memory abilities in Alzheimer's disease (Qu, Xiong, Hujie et al., 2021). Alzheimer's disease and PD, both belonging to neuro-degenerative disease, the former is a neurodegenerative brain pathology formed due to piling up of amyloid proteins, development of plaques and disappearance of neurons (Tufail, Ma, Zhang et al., 2021).while the latter is caused by the loss of dopaminergic neurons in the substantia nigra (Xu, Zhang, Kang et al.,

2021). On parallel, the treatment strategies between our two literatures were also different. In our study, LPS induced BV-2 cells were used as inflammatory cell models and the supernatant of BV-2 cell was co-cultured with SH-SY5Y cells. As for the PD rat models, MPTP treatment was given to rats for consecutively 5 days. This discrepancy may be explained by the difference on the disease background and treatment strategy. Similar to our detection, previous studies identified that miR-132-3p was one of the upregulated cimiRNAs in patients with major depression disorder (van den Berg, Krauskopf, Ramaekers et al., 2020). and was found to be elevated in the serum of patients with mild cognitive impairment (Xie, Zhou, Zhang et al., 2015). In addition, we also revealed that GLRX suppresses activation of microglial cells and ameliorates neuronal injury caused by *miR-132-3p*. Finally, we found that MPTP-induced neuroinflammation and degeneration of dopaminergic neurons in PD mouse models are dramatically attenuated after *miR-132-3p* downregulation. Thus, our study not only uncovered novel roles for *miR-132-3p* and GLRX in the pathological abnormalities related to PD but also identified their potential application in the treatment for PD.

Microglial cells are macrophages residing in the brain, which originate from early erythro-myeloid precursors in the embryonic yolk sac (Kanthasamy, Jin, Charli et al., 2019). Activated microglial cells at the inflammation site promote the release of inflammatory cytokines, thereby intensifying the inflammatory response through activation and recruitment of other cells to the brain lesion (Kim & Joh, 2006). Accumulating evidence proposed that in the process of PD, microglial cells are activated, and then trigger the secretion of a variety of pro-inflammatory factors, including IL-6, IL-1β and TNF-α (Guan, Yang, Fan et al., 2017). In an attempt to elucidate the mechanism by which *miR-132-3p* accelerates the progression of PD, we

first investigated whether *miR-132-3p* affects the activation of microglial cells. Initially, remarkable high expression pattern of *miR-132-3p* was noticed in midbrain tissues from patients with PD rather than tissues of healthy controls. To this end, LPS was applied to simulate the inflammatory response in BV-2 cells. Herein, results of gain-and loss-of-function experiments confirmed that *miR-132-3p* might likewise contribute to the activation of microglial cells. In our study, knockdown of miR-132-3p can suppress the release of inflammatory cytokines, including TNF-α, IL-1β and IL-6, while overexpression of miR-132-3p can promote the inflammatory response in BV-2 cells, those results indicated that miR-132 as a driver of microglia pro-inflammatory responses. Of note, there has been relevant evidence supporting our findings that *miR-132* confers a pivotal role in intracerebral hemorrhage by regulating inflammation, which is evident from the activation state of microglial cells and the expression of pro-inflammatory cytokines (Zhang, Han, He et al., 2017). Furthermore, by using CCK-8 assay and flow cytometry, we discovered that LPS can suppress survival rate of microglial cells and increase cell apoptosis, while further treatment by *miR-132-3p* knockdown partially reverse the LPS induced cell apoptosis and elevate cell survival rate to certain extent. Further measurement showed that activated microglial cells by *miR-132-3p* may lead to neuronal injury, as evidenced by reinforced cell apoptotic ability and reduced the proliferative ability of SH-SY5Y cells after SH-SY5Y cells were cultured with the conditioned medium of BV-2 cells which were transfected with *miR-132-3p* mimic, which highlighted the role of *miR-132-3p* in activation of microglial cells and neuronal injury. Interestingly, former work described that the dysregulation of *miR-132* leads to the occurrence and exacerbation of PD (Qian, Song, Ouyang et al., 2017). The BACE1-AS/*miR-132-3p* axis is responsible for the berberine-mitigated neuronal injury in Alzheimer's disease

(Ge, Song, Liu et al., 2020). Therefore, *miR-132-3p* may exert a negative effect on PD by inducing neuroinflammation and neuronal injury.

Subsequently, we are prompted to further look into the molecular actions of *miR-132-3p* in regulating PD by investigating the downstream target. Based on the comprehensive analysis from StarBase, dual-luciferase reporter assay and RIP assay, we identified GLRX as a direct target of *miR-132-3p*. GLRX is an indispensable thioltransferase whose main function is to remove protein glutathionylation (Burns, Rizvi, Tsukahara et al., 2020). Herein, the lowly expressed GLRX was observed in the midbrain tissues of PD patients. Furthermore, analyses of qRT-PCR, Western blot, ELISA, CCK-8 assay and flow cytometry elaborated that *miR-132-3p* interfered with microglial activation and neuronal injury by targeting GLRX. Our data are in agreement with the earlier findings showing that enhancement of GLRX activity in these brain cells would impede the progression of PD (Gorelenkova Miller & Mieyal, 2019). MPTP is a neurotoxin that results in a profound reduction of striatal dopamine levels and specific loss of dopaminergic neurons in animals (Lee, Hwang, Park et al., 2019). To further shed light into the relationship between *miR-132-3p*/GLRX and PD, we used a mouse model of PD stimulated by MPTP. Consistently, mice received MPTP injection had increased inflammatory cytokine release and decreased TH positive neurons, indicating the neuron loss in MPTP treated mice. On parallel, elevated *miR-132-3p* expression and decreased expression of GLRX were also observed in mice in MPTP group, suggesting the possible implication of *miR-132-3p* in neuron loss of PD mouse. Here, we showed that *miR-132-3p* downregulation in PD mouse induces alterations in GLRX expression, and *miR-132-3p* was responsible for the inflammatory response of brain tissues of PD mouse models by modulating GLRX. Additionally, immunofluorescence of Iba1 on detection of microglial activation and

612 immunofluorescence of tyrosine hydroxylase on assessment of dopaminergic neuron
613 loss revealed that depletion of *miR-132-3p* may alleviate MPTP-induced
614 dopaminergic neurodegeneration and neuroinflammation of PD mouse models.
615 Simultaneously, these findings were further supported by the rotarod test and open
616 field test.

617 In conclusion, our data suggest that the deficiency of *miR-132-3p* contributes to
618 ameliorated PD. *MiR-132-3p* enhances the activation of microglia cells and promotes
619 the release of inflammatory cytokines by targeting GLRX to exert toxic effect on
620 neurons. These findings suggest that targeting neuroprotective pathways controlled by
621 *miR-132-3p* may represent a potential therapeutic intervention strategy for PD therapy.
622 Further work is required to ascertain whether the protection from PD observed here
623 by silencing of the *miR-132-3p* is exerted by GLRX, inhibition of microglial
624 activation and dopaminergic neuron loss or perhaps via modulation of other pathways.
625

Acknowledgement

Thanks for all the contributors and participants.

Conflict of interests

The authors declare there is no conflict of interests.

Funding

This research was funded by the grants from Hunan Provincial Natural Science Foundation (Grant No. 2019JJ50322) and the Science Research Planning Program of Health and Family Planning Commission of Hunan Province (Grant No. C2019054).

References

R Alizadeh, S K Kamrava, Z Bagher, M Farhadi, M Falah, F Moradi, M E Boroujeni, M Soleimani, A Kamyab, & A Komeili. (2019). Human olfactory stem cells: As a promising source of dopaminergic neuron-like cells for treatment of Parkinson's disease. *Neurosci Lett, 696*, 52-59. doi:10.1016/j.neulet.2018.12.011

E Angelopoulou, Y N Paudel, & C Piperi. (2019). miR-124 and Parkinson's disease: A biomarker with therapeutic potential. *Pharmacol Res, 150*, 104515. doi:10.1016/j.phrs.2019.104515

T B Bassani, M A Vital, & L K Rauh. (2015). Neuroinflammation in the pathophysiology of Parkinson's disease and therapeutic evidence of anti-inflammatory drugs. *Arq Neuropsiquiatr, 73*(7), 616-623. doi:10.1590/0004-282X20150057

M Burns, S H M Rizvi, Y Tsukahara, D R Pimentel, I Luptak, N M Hamburg, R Matsui, & M M Bachschmid. (2020). Role of Glutaredoxin-1 and Glutathionylation in Cardiovascular Diseases. *Int J Mol Sci, 21*(18). doi:10.3390/ijms21186803

Y Ge, X Song, J Liu, C Liu, & C Xu. (2020). The Combined Therapy of Berberine Treatment with lncRNA BACE1-AS Depletion Attenuates Abeta25-35 Induced Neuronal Injury Through Regulating the Expression of miR-132-3p in Neuronal Cells. *Neurochem Res, 45*(4), 741-751. doi:10.1007/s11064-019-02947-6

O Gorelenkova Miller, & J J Mieyal. (2019). Critical Roles of Glutaredoxin in Brain Cells-Implications for Parkinson's Disease. *Antioxid Redox Signal, 30*(10), 1352-1368. doi:10.1089/ars.2017.7411

J Guan, B Yang, Y Fan, & J Zhang. (2017). GPER Agonist G1 Attenuates Neuroinflammation and Dopaminergic Neurodegeneration in Parkinson Disease. *Neuroimmunomodulation, 24*(1), 60-66. doi:10.1159/000478908

E C Hirsch, & S Hunot. (2009). Neuroinflammation in Parkinson's disease: a target for neuroprotection? *Lancet Neurol, 8*(4), 382-397. doi:10.1016/S1474-4422(09)70062-6

Y B Hu, Y F Zhang, H Wang, R J Ren, H L Cui, W Y Huang, Q Cheng, H Z Chen, & G Wang. (2019). miR-425 deficiency promotes necroptosis and dopaminergic neurodegeneration in Parkinson's disease. *Cell Death Dis, 10*(8), 589. doi:10.1038/s41419-019-1809-5

Z J. (2020). Brain gamma rhythm and potential treatment of neurodegenerative disease. *Journal of Neurorestoratolog, 8*(1), 26-31.

Y F Ji, D Wang, Y R Liu, X R Ma, H Lu, & B A Zhang. (2018). MicroRNA-132 attenuates LPS-induced inflammatory injury by targeting TRAF6 in neuronal cell line HT-22. *J Cell Biochem, 119*(7), 5528-5537. doi:10.1002/jcb.26720

W M Johnson, C Yao, S L Siedlak, W Wang, X Zhu, G A Caldwell, A L Wilson-Delfosse, J J Mieyal, & S G Chen. (2015). Glutaredoxin deficiency exacerbates neurodegeneration in C. elegans models of Parkinson's disease. *Hum Mol Genet, 24*(5), 1322-1335. doi:10.1093/hmg/ddu542

A Kanthasamy, H Jin, A Charli, A Vellareddy, & A Kanthasamy. (2019). Environmental neurotoxicant-induced dopaminergic neurodegeneration: a potential link to impaired neuroinflammatory mechanisms. *Pharmacol Ther, 197*, 61-82. doi:10.1016/j.pharmthera.2019.01.001

Y S Kim, & T H Joh. (2006). Microglia, major player in the brain inflammation: their roles in the pathogenesis of Parkinson's disease. *Exp Mol Med, 38*(4), 333-347.

doi:10.1038/emm.2006.40

P Krashia, A Cordella, A Nobili, L La Barbera, M Federici, A Leuti, F Campanelli, G Natale, G Marino, V Calabrese, F Vedele, V Ghiglieri, B Picconi, G Di Lazzaro, T Schirinzi, G Sancesario, N Casadei, O Riess, S Bernardini, A Pisani, P Calabresi, M T Viscomi, C N Serhan, V Chiurchiu, M D'Amelio, & N B Mercuri. (2019). Blunting neuroinflammation with resolvin D1 prevents early pathology in a rat model of Parkinson's disease. *Nat Commun, 10*(1), 3945. doi:10.1038/s41467-019-11928-w

E Lee, I Hwang, S Park, S Hong, B Hwang, Y Cho, J Son, & J W Yu. (2019). MPTP-driven NLRP3 inflammasome activation in microglia plays a central role in dopaminergic neurodegeneration. *Cell Death Differ, 26*(2), 213-228. doi:10.1038/s41418-018-0124-5

M Leinders, N Uceyler, R A Pritchard, C Sommer, & L S Sorkin. (2016). Increased miR-132-3p expression is associated with chronic neuropathic pain. *Exp Neurol, 283*(Pt A), 276-286. doi:10.1016/j.expneurol.2016.06.025

N Li, X Pan, J Zhang, A Ma, S Yang, J Ma, & A Xie. (2017). Plasma levels of miR-137 and miR-124 are associated with Parkinson's disease but not with Parkinson's disease with depression. *Neurol Sci, 38*(5), 761-767. doi:10.1007/s10072-017-2841-9

M E Lull, & M L Block. (2010). Microglial activation and chronic neurodegeneration. *Neurotherapeutics, 7*(4), 354-365. doi:10.1016/j.nurt.2010.05.014

B P Mead, N Kim, G W Miller, D Hodges, P Mastorakos, A L Klibanov, J W Mandell, J Hirsh, J S Suk, J Hanes, & R J Price. (2017). Novel Focused Ultrasound Gene Therapy Approach Noninvasively Restores Dopaminergic Neuron Function in a Rat Parkinson's Disease Model. *Nano Lett, 17*(6), 3533-3542. doi:10.1021/acs.nanolett.7b00616

C Milanese, S Gabriels, S Barnhoorn, S Cerri, A Ulusoy, S V Gornati, D F Wallace, F Blandini, D A Di Monte, V N Subramaniam, & P G Mastroberardino. (2020). Gender biased neuroprotective effect of Transferrin Receptor 2 deletion in multiple models of Parkinson's disease. *Cell Death Differ*. doi:10.1038/s41418-020-00698-4

R B Postuma, W Poewe, I Litvan, S Lewis, A E Lang, G Halliday, C G Goetz, P Chan, E Slow, K Seppi, E Schaffer, S Rios-Romenets, T Mi, C Maetzler, Y Li, B Heim, I O Bledsoe, & D Berg. (2018). Validation of the MDS clinical diagnostic criteria for Parkinson's disease. *Mov Disord, 33*(10), 1601-1608. doi:10.1002/mds.27362

T J Qazi, J Lu, L Duru, J Zhao, & H Qing. (2021). Upregulation of mir-132 induces dopaminergic neuronal death via activating SIRT1/P53 pathway. *Neurosci Lett, 740*, 135465. doi:10.1016/j.neulet.2020.135465

Y Qian, J Song, Y Ouyang, Q Han, W Chen, X Zhao, Y Xie, Y Chen, W Yuan, & C Fan. (2017). Advances in Roles of miR-132 in the Nervous System. *Front Pharmacol, 8*, 770. doi:10.3389/fphar.2017.00770

J Qu, X Xiong, G Hujie, J Ren, L Yan, & L Ma. (2021). MicroRNA-132-3p alleviates neuron apoptosis and impairments of learning and memory abilities in Alzheimer's disease by downregulation of HNRNPU stabilized BACE1. *Cell Cycle*, 1-12. doi:10.1080/15384101.2021.1982507

A M Strubberg, & B B Madison. (2017). MicroRNAs in the etiology of colorectal cancer: pathways and clinical implications. *Dis Model Mech, 10*(3), 197-214. doi:10.1242/dmm.027441

S Sveinbjornsdottir. (2016). The clinical symptoms of Parkinson's disease. *J Neurochem, 139 Suppl 1*, 318-324. doi:10.1111/jnc.13691

A B Tufail, Y K Ma, Q N Zhang, A Khan, L Zhao, Q Yang, M Adeel, R Khan, & I Ullah. (2021). 3D

convolutional neural networks-based multiclass classification of Alzheimer's and Parkinson's diseases using PET and SPECT neuroimaging modalities. *Brain Inform, 8*(1), 23. doi:10.1186/s40708-021-00144-2

M M J van den Berg, J Krauskopf, J G Ramaekers, J C S Kleinjans, J Prickaerts, & J J Briede. (2020). Circulating microRNAs as potential biomarkers for psychiatric and neurodegenerative disorders. *Prog Neurobiol, 185*, 101732. doi:10.1016/j.pneurobio.2019.101732

A Verma, A Ray, D Bapat, L Diwakar, R P Kommaddi, B L Schneider, E C Hirsch, & V Ravindranath. (2020). Glutaredoxin 1 Downregulation in the Substantia Nigra Leads to Dopaminergic Degeneration in Mice. *Mov Disord, 35*(10), 1843-1853. doi:10.1002/mds.28190

L Wang, J Liu, J Liu, X Chen, M Chang, J Li, J Zhou, C Bai, & Y Song. (2019). GLRX inhibition enhances the effects of geftinib in EGFR-TKI-resistant NSCLC cells through FoxM1 signaling pathway. *J Cancer Res Clin Oncol, 145*(4), 861-872. doi:10.1007/s00432-019-02845-y

B Xie, H Zhou, R Zhang, M Song, L Yu, L Wang, Z Liu, Q Zhang, D Cui, X Wang, & S Xu. (2015). Serum miR-206 and miR-132 as Potential Circulating Biomarkers for Mild Cognitive Impairment. *J Alzheimers Dis, 45*(3), 721-731. doi:10.3233/JAD-142847

X Xu, Y Zhang, Y Kang, S Liu, Y Wang, Y Wang, & L Wang. (2021). LncRNA MIAT Inhibits MPP(+)-Induced Neuronal Damage Through Regulating the miR-132/SIRT1 Axis in PC12 Cells. *Neurochem Res, 46*(12), 3365-3374. doi:10.1007/s11064-021-03437-4

Z Yang, T Li, S Li, M Wei, H Qi, B Shen, R C Chang, W Le, & F Piao. (2019). Altered Expression Levels of MicroRNA-132 and Nurr1 in Peripheral Blood of Parkinson's Disease: Potential Disease Biomarkers. *ACS Chem Neurosci, 10*(5), 2243-2249. doi:10.1021/acschemneuro.8b00460

Y Ye, X He, F Lu, H Mao, Z Zhu, L Yao, W Luo, X Sun, B Wang, C Qian, Y Zhang, G Lu, & S Zhang. (2018). A lincRNA-p21/miR-181 family feedback loop regulates microglial activation during systemic LPS- and MPTP- induced neuroinflammation. *Cell Death Dis, 9*(8), 803. doi:10.1038/s41419-018-0821-5

Y Zhang, B Han, Y He, D Li, X Ma, Q Liu, & J Hao. (2017). MicroRNA-132 attenuates neurobehavioral and neuropathological changes associated with intracerebral hemorrhage in mice. *Neurochem Int, 107*, 182-190. doi:10.1016/j.neuint.2016.11.011

Legends

Figure 1 Expressions of *miR-132-3p* and GLRX in the midbrain tissues of patients with PD

Note: The mRNA expression of *miR-132-3p* in the midbrain tissues of 5 PD patients and 5 age-matched controls was detected by qRT-PCR (A), and the mRNA and protein expressions of GLRX were measured by qRT-PCR (B) and Western blot (C); N (number of participants) = 5, $^{*}P < 0.05$, $^{**}P < 0.01$; PD, Parkinson's disease.

Figure 2 LPS-induced inflammatory response in BV-2 microglial cells can be attenuated by *miR-132-3p* knockdown

Notes: Following transfection with *miR-132-3p* inhibitor or inhibitor NC, BV-2 cells were treated with 0.1 μg/mL LPS or PBS for 24 h. qRT-PCR was used to detect the expression of *miR-132-3p* in BV-2 cells (A). The mRNA expressions of inflammatory cytokines TNF-α, IL-1β and IL-6 were analyzed by qRT-PCR (B), and the contents of TNF-α, IL-1β and IL-6 in the supernatant of BV-2 cells were determined by ELISA (C); N (number of independent cell culture preparations) =3, $^{**}P < 0.01$, $^{***}P < 0.001$; LPS, lipopolysaccharide.

Figure 3 Overexpression of *miR-132-3p* promotes the release of pro-inflammatory cytokines in BV-2 microglial cells

Notes: After BV-2 cells transfected with *miR-132-3p* mimic or mimic NC, the mRNA expression of *miR-132-3p* in BV-2 cells (A) and the mRNA expressions of inflammatory cytokines TNF-α, IL-1β and IL-6 in BV-2 cells were examined by qRT-PCR (B). Then, ELISA was utilized to assess the contents of TNF-α, IL-1β and IL-6 in the supernatant of BV-2 cells (C); N (number of independent cell culture preparations) = 3, $^{**}P < 0.01$, $^{***}P < 0.001$.

Figure 4 Effect of *miR-132-3p* induced microglial activation on neuronal injury

Notes: The SH-SY5Y cells were cultured in the conditioned medium of BV-2 cells that were transfected with inhibitor NC or *miR-132-3p* inhibitor and stimulated with LPS. Then, CCK-8 assay was used to detect the viability of SH-SY5Y cells (A) and flow cytometry to determine the apoptotic rate (B). Additionally, SH-SY5Y cells were cultured in the conditioned medium of BV-2 cells that transfected with *miR-132-3p* mimic or mimic NC. The viability of SH-SY5Y cells was assessed by CCK-8 assay (C) and the apoptotic rate of SH-SY5Y cells was measured by flow cytometry (D); N (number of independent cell culture preparations) = 3, $^{*}P < 0.05$, $^{**}P < 0.01$, $^{***}P < 0.001$.

Figure 5 *MiR-132-3p* negatively mediates GLRX

Notes: qRT-PCR (A) and Western blot (B) were used to detect the mRNA and protein expressions of GLRX after *miR-132-3p* knockdown or overexpression in BV-2 cells. RIP experiment was applied to verify the binding of *miR-132-3p* to GLRX mRNA (C). After LPS or PBS treatment, RIP was applied to detect the GLRX mRNA expression in Ago2 complex (D). The binding site of *miR-132-3p* to the 3'-UTR of GLRX mRNA was predicted by StarBase (E). Dual-luciferase reporter assay was utilized to verify the binding relationship between *miR-132-3p* and GLRX (F); N (number of independent cell culture preparations) = 3, $^{*}P < 0.05$, $^{**}P < 0.01$, $^{***}P < 0.001$; UTR, untranslated region.

Figure 6 GLRX reverses microglial activation and neuronal injury induced by *miR-132-3p*

Notes: The BV-2 cells were transfected *miR-132-3p* mimic or co-transfected *miR-132-3p* mimic and GLRX overexpressing plasmid. Then, qRT-PCR (A) and Western blot (B) were used to detect the mRNA and protein expressions of GLRX in BV-2 cells. The mRNA expressions of inflammatory cytokines TNF-α, IL-1β and IL-6

in BV-2 cells were examined by qRT-PCR (C). Then, ELISA was utilized to assess the contents of TNF-α, IL-1β and IL-6 in the supernatant of BV-2 cells (D). The SH-SY5Y cells were cultured in conditioned medium, in which BV-2 cells were transfected with *miR-132-3p* mimic or co-transfected *miR-132-3p* mimic and GLRX overexpressing plasmid. Then, CCK-8 assay was used to detect the viability of SH-SY5Y cells (E) and flow cytometry to determine the apoptotic rate (F); N (number of independent cell culture preparations) = 3, $^{*}P < 0.05$, $^{**}P < 0.01$, $^{***}P < 0.001$.

Figure 7 Knockdown of *miR-132-3p* ameliorates the neuroinflammation and dopaminergic neuron degeneration of PD mouse

Notes: Mice were intraperitoneally injected with 30 mg/kg MPTP to establish PD mouse models. Then, mouse models of PD were given stereotactic injection of *miR-132-3p* antagomir or antagomir NC. FISH was used to examine the expression of *miR-132-3p* in SNc of mice (A). The expression of GLRX in the SNc of mice was measured by immunohistochemistry (B). FISH was applied to detect the expression of miR-132-3p in microglial cells (C). Immunofluorescence was applied to detect the expression of GLRX in microglial cells (D); Immunofluorescence of Iba1 was applied to detect the activation of microglial cells (E), qRT-PCR to detect the mRNA expressions of TNF-α, IL-1β and IL-6 in brain tissues of mouse (F), and immunofluorescence of tyrosine hydroxylase to detect the loss of dopaminergic neurons in the SNc of mice (G). The motor ability of mice was assessed after rotarod test and open field test (H); N (number of animals) = 6, $^{*}P < 0.05$, $^{**}P < 0.01$, $^{***}P < 0.001$; PD, Parkinson's disease; FISH, fluorescence in situ hybridization; SNc, substantia nigra pars compacta.

Table 1 Primer sequence information

Notes: F: forward primer; R: reverse primer.

Table 2. Abbreviation list.

Table 3. Reagents and materials.

Table 4. Statistical summary and analysis methods

Table 1 Primer sequence information

Name of primer	Sequences
U6-F	CTCGCTTCGGCAGCACA
U6-R	AACGCTTCACGAATTTGCGT
miR-132-3p -F	GCTGGTACCGACATCT
miR-132-3p -R	TGGTGTCGTGGAGTCG
β-actin-F	GAAGGCTATAGTCACCTCGGG
β-actin-R	ATGGTAATAATGCGGCCGGT
GLRX-F	GGGTTGGGGTGATTTGAGGA
GLRX-R	TCCTTAGGCAACGTCCAACA
TNF-α-F	ACTGATGAGAGGGAGGCCAT
TNF-α-R	CCGTGGGTTGGACAGATGAA
IL-1β-F	GGGGCGTCCTTCATATGTGT
IL-1β-R	ATACAACGGCTCCTCCGTTC
IL-6-F	TGCTTCCCCATCTCTCATGC
IL-6-R	TGTCTGGAAAAAGTGCCGCT

Notes: F: forward primer; R: reverse primer.

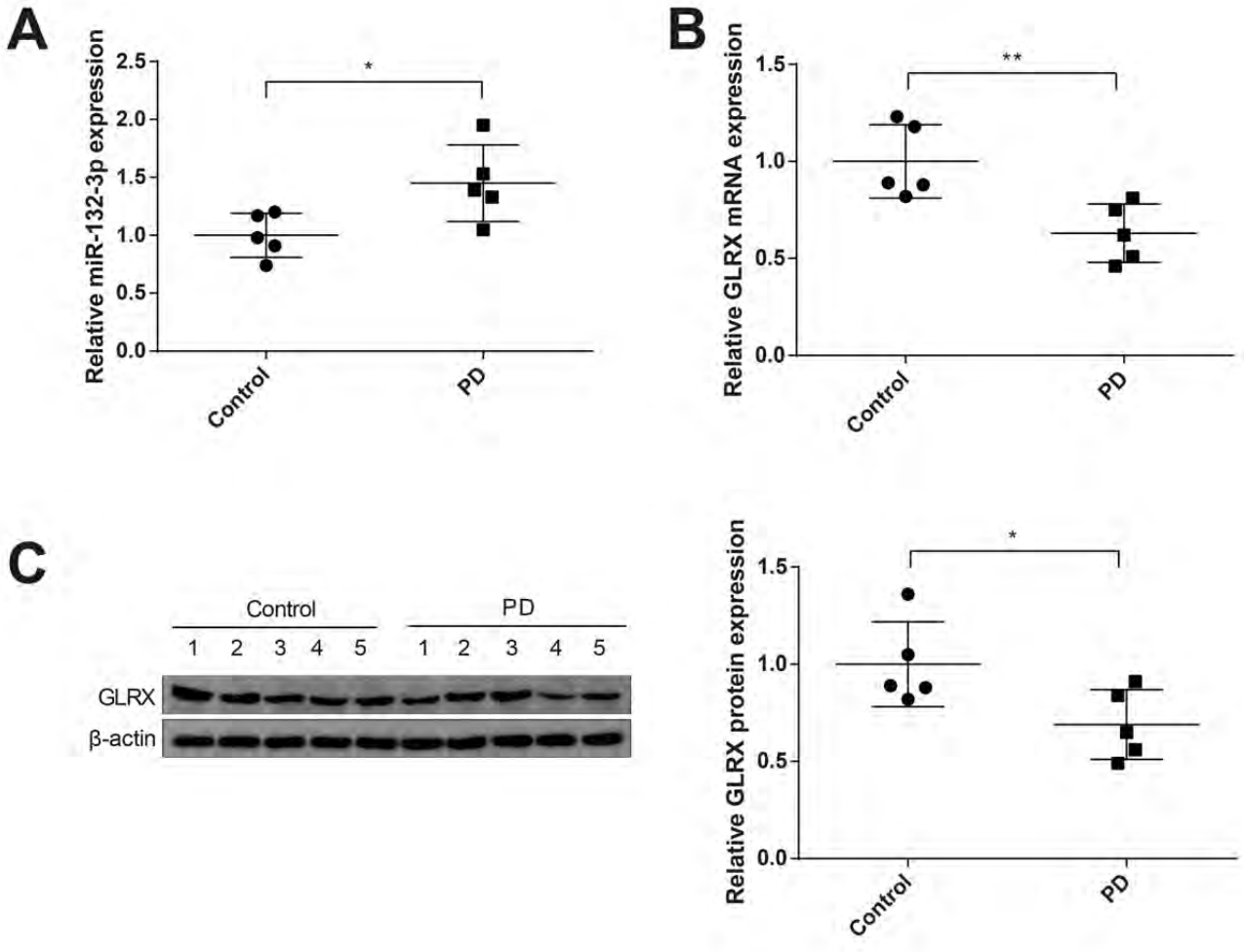

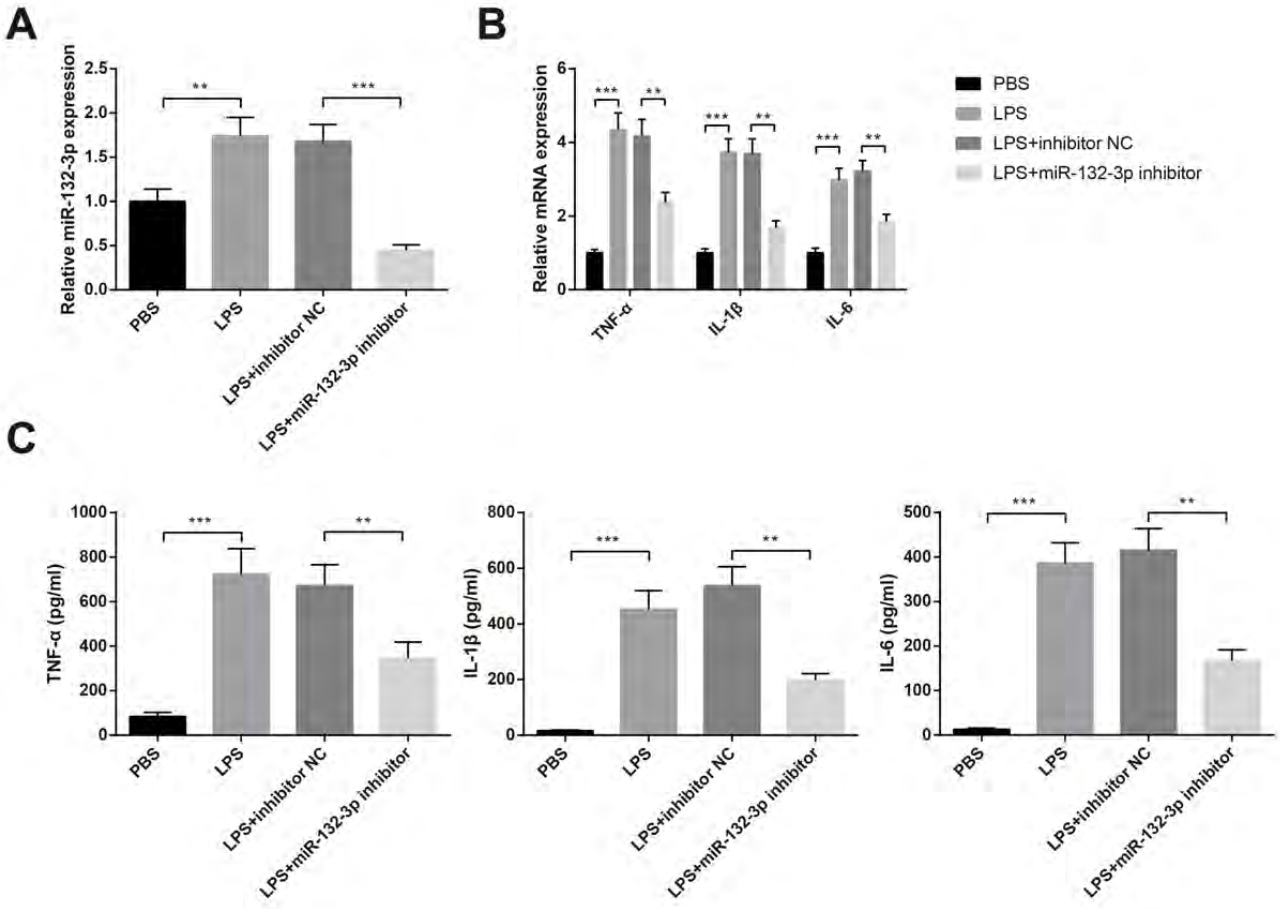

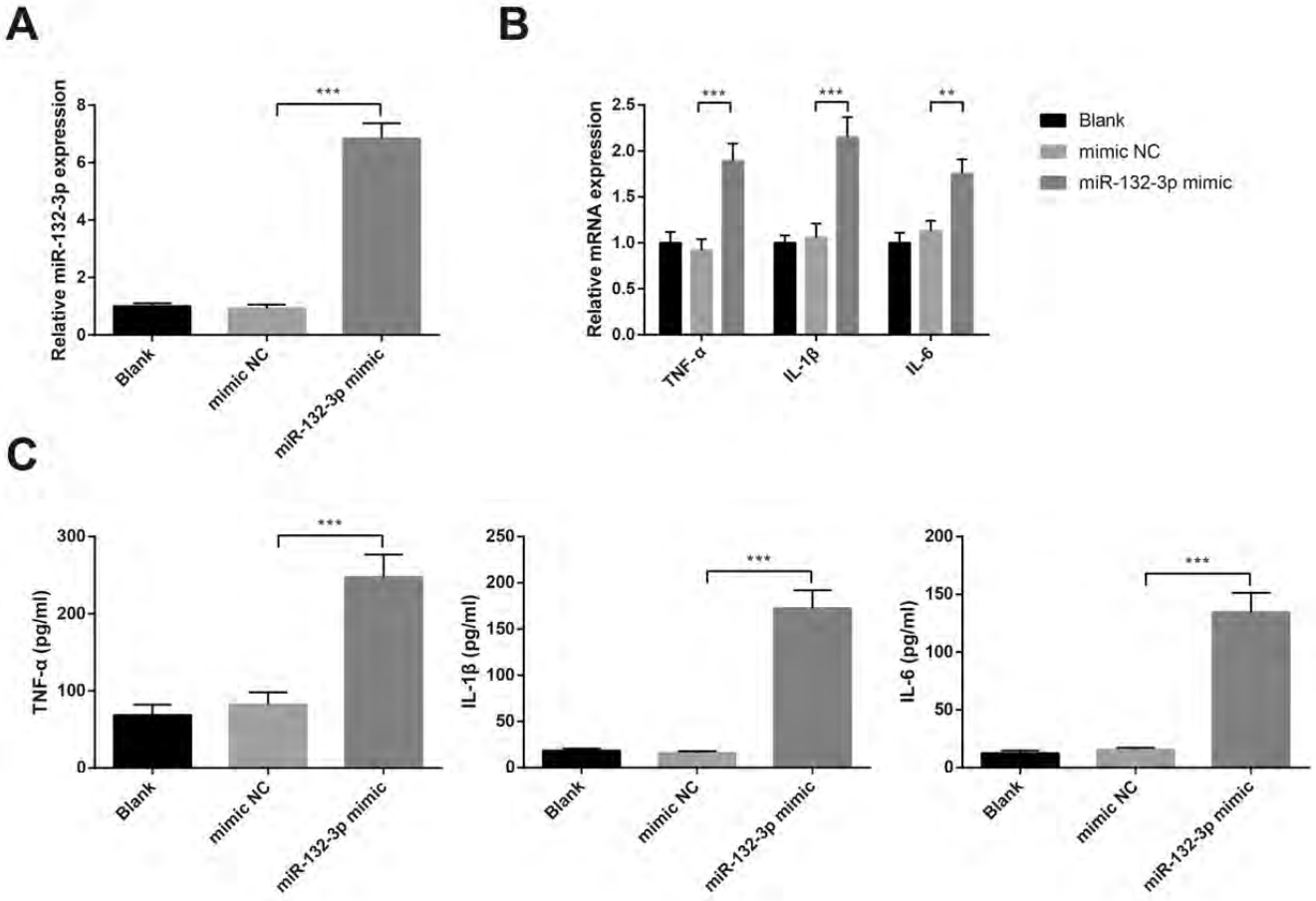

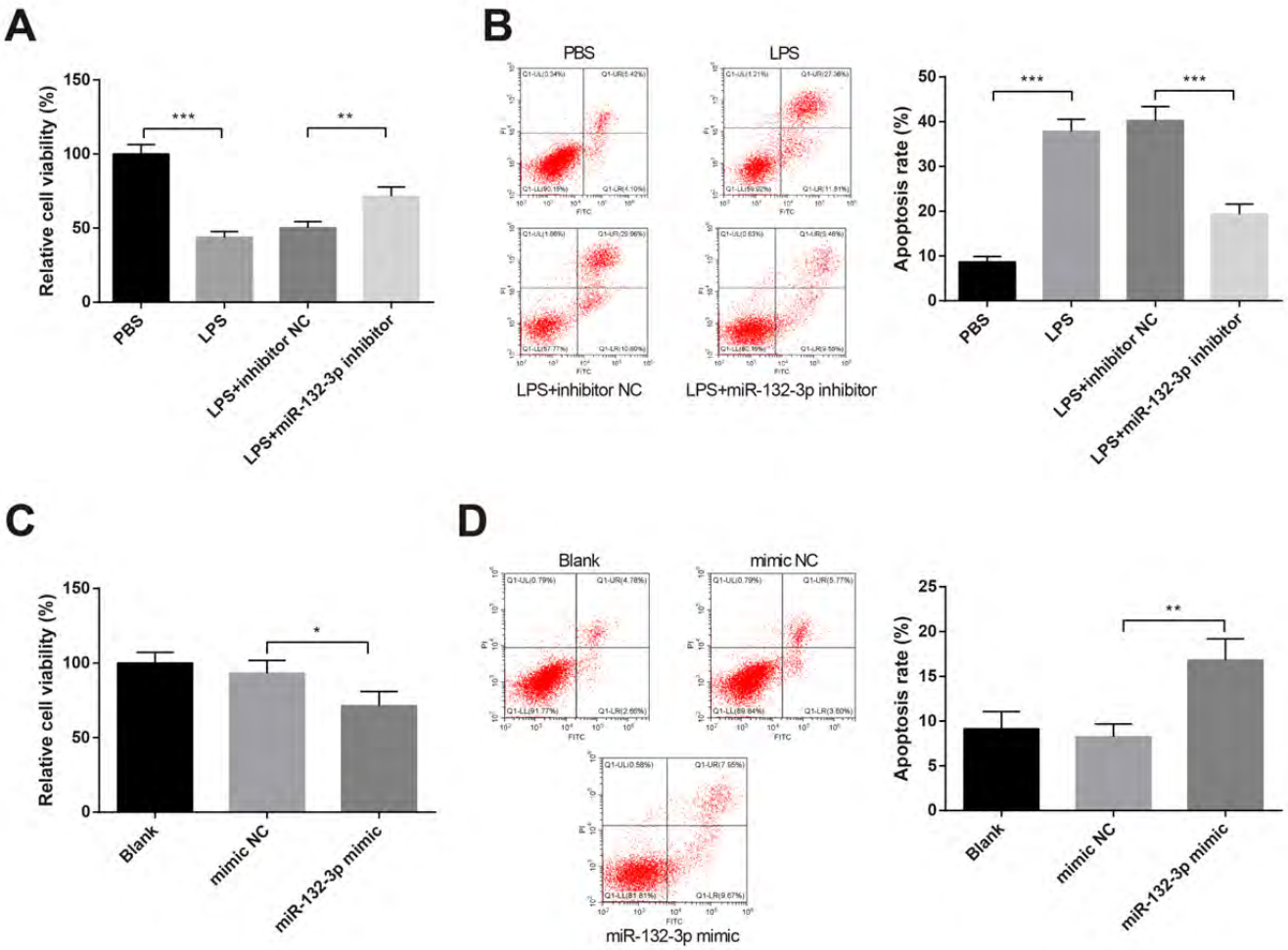

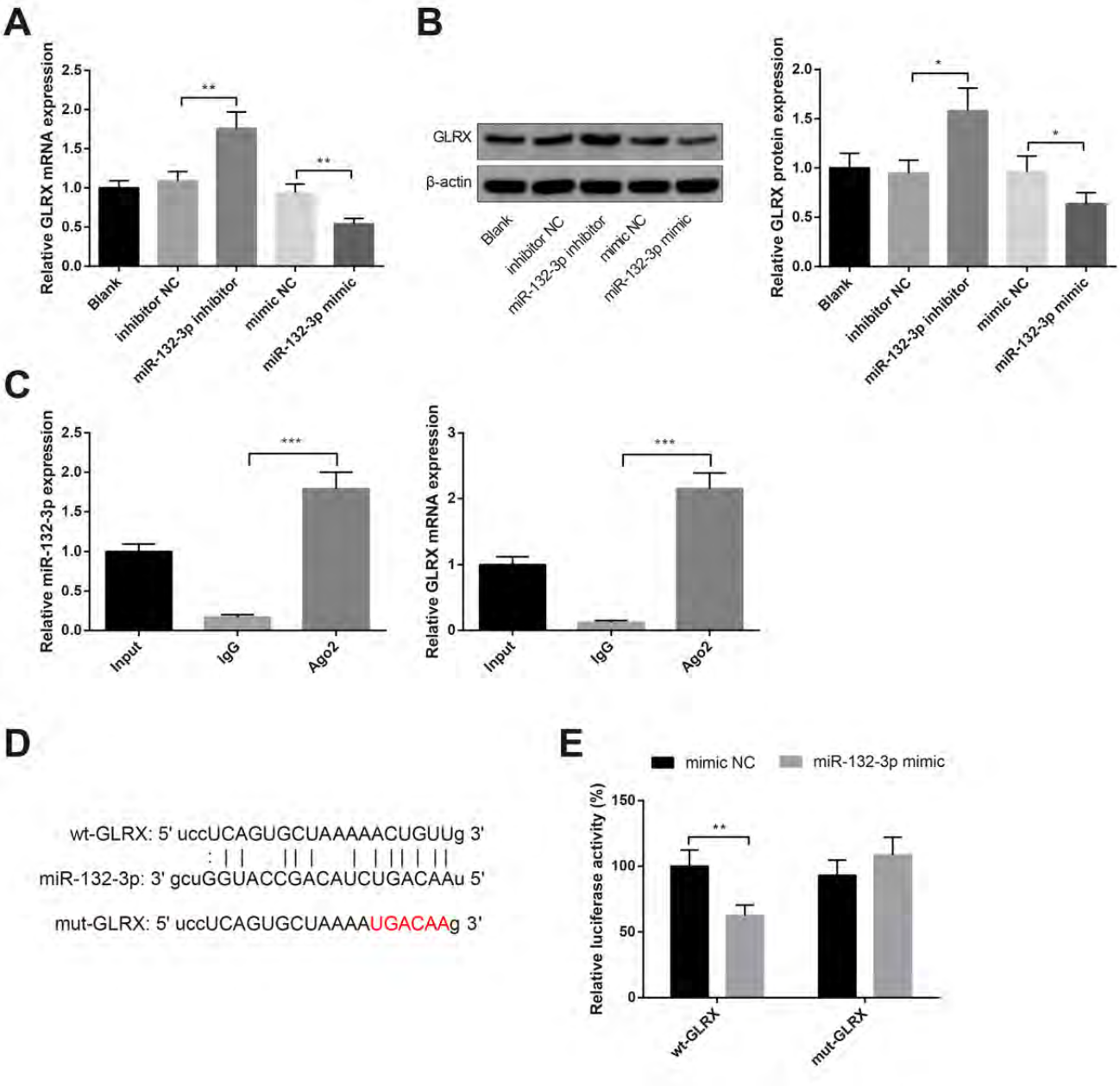

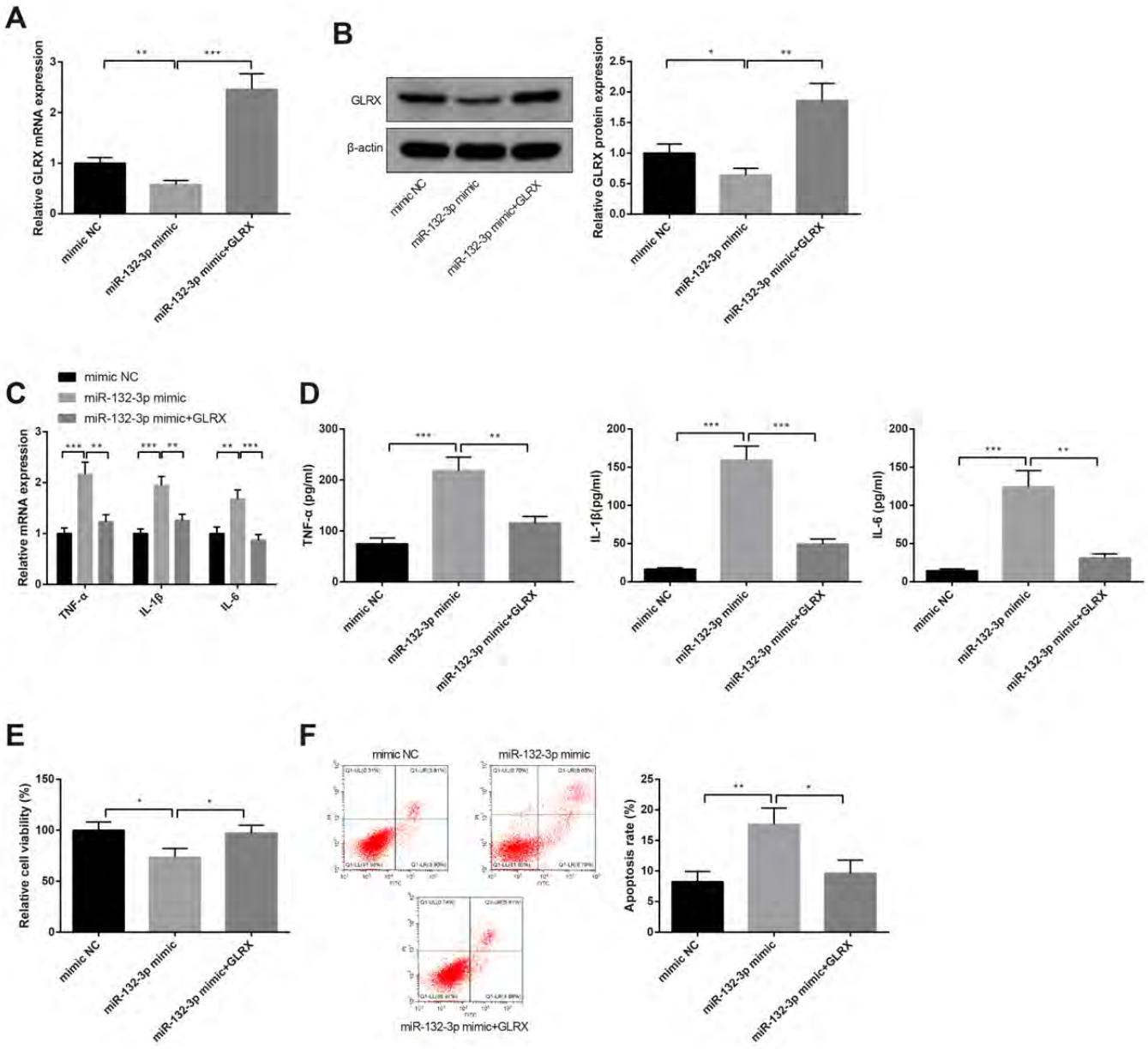

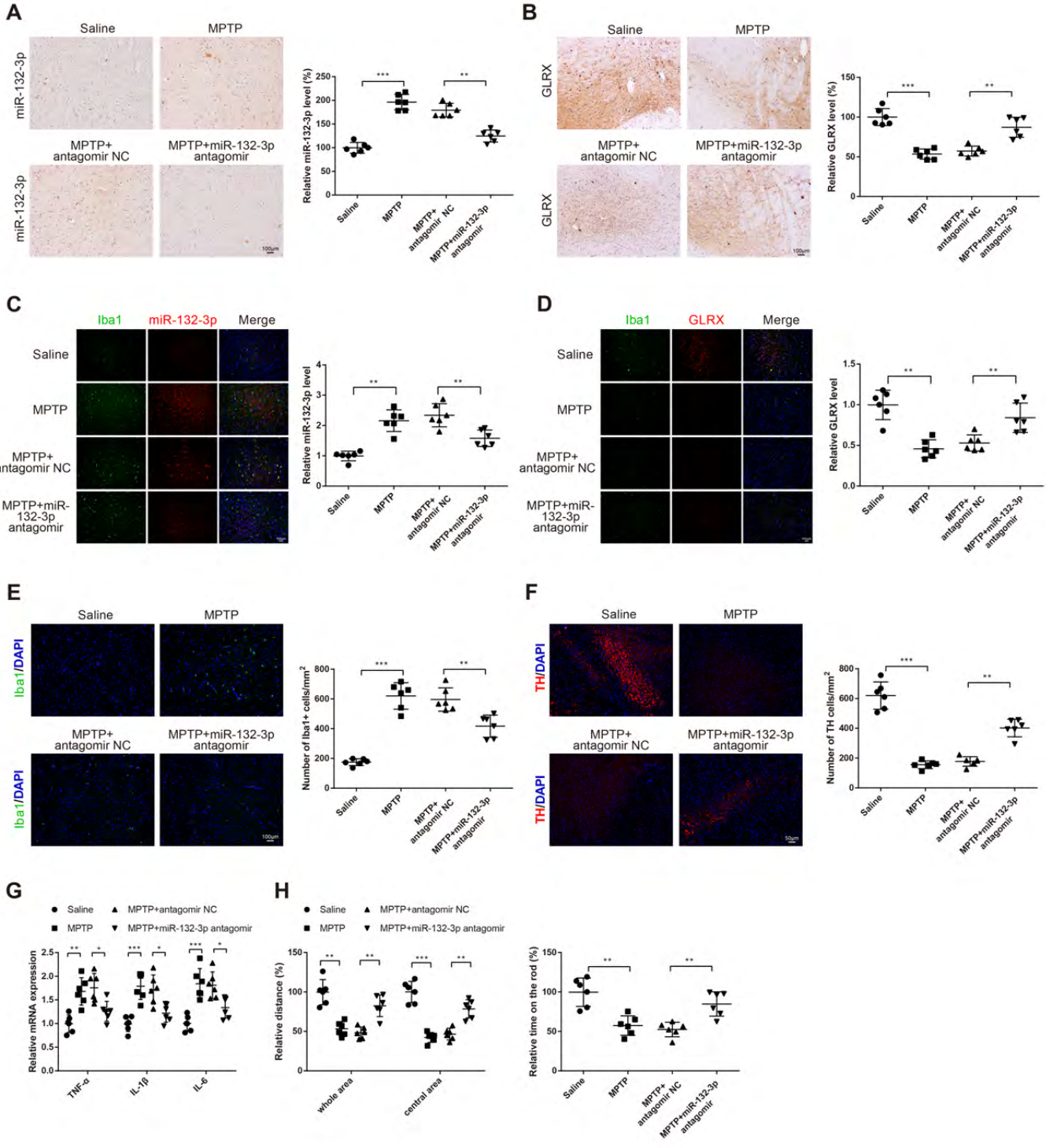

Table 2. Abbreviation list.

Abbreviations	Full names
PD	Parkinson's disease
GLRX	Glutaredoxin
LPS	Lipopolysaccharide
qRT-RCR	Quantitative Real-time polymerase chain reaction
ELISA	enzyme-linked immunosorbent assay
RIP	RNA immunoprecipitation
MPTP	1-methyl-4-phenyl-1, 2, 3, 6-tetrahydropyridine
SNc	substantia nigra compacta
TH	tyrosine hydroxylase
DMEM	dulbecco's modified eagle medium
PBS	phosphate buffer
Ago2	Argonaute 2
FBS	fetal bovine serum
FITC	fluorescein isothiocyanate
PI	propidium iodide
FISH	Fluorescence in situ hybridization
RRID	Research Resource Identifier

Table 3. Reagents and materials.

Names	RRIDs or catalogue number
BV-2 cell	Cat# YB-ATCC-4255, ATCC
SH-SY5Y cell	RRID:CVCL_0019
HEK293T cell	RRID:CVCL_0063
DMEM	Cat# 11054001, Gibco
DMEM/F12	Cat# 11330107, Gibco
FBS	Cat# 16140, Invitrogen
Penicillin/streptomycin	Cat# 15140148, Invitrogen
LPS	Cat# L-4391, Sigma-Aldrich
Lipofectamine 3000	Cat# L3000150, Invitrogen
TRIZOL	Cat# 15596026, Invitrogen
Reverse transcription kit	Cat# 6210A, TaKaRa
SYBR Green Mix	Cat# 2015099, Roche
RIPA lysis buffer	Cat# P0013C, Beyotime
BCA kit	Cat# P0012, Beyotime
Protein loading buffer	Cat# P0015A, Beyotime
β-actin antibody	RRID:AB_306371
GLRX antibody	RRID:AB_880242
Film Development Kit	Cat# P0019, Beyotime
TNF-α	Cat# DY410, R&D
IL-1β	Cat# SMLB00C, R&D
IL-6	Cat# SM6000B, R&D
CCK-8 kit	Cat# CK04, Dojindo
Annexin V-FITC cell apoptosis kit	Cat# C1062L, Beyotime
PBS	Cat# C0221A, Beyotime
A+G beads	Cat# P2108, Beyotime
Ago2 antibody	RRID:AB_867543
IgG antibody	RRID:AB_2687931
pGL3-Promoter	Cat# E1761, Promega
pRL-TK	Cat# E2241, Promega

Dual-Luciferase® Reporter Assay System	Cat# E1910, Promega
MPTP	Cat# M0896, Sigma-Aldrich
4% paraformaldehyde	Cat# P0099, Beyotime
Proteinase K	Cat# ST535, Beyotime
Tyrosine Hydroxylase antibody	RRID:AB_2801410
Iba1 antibody	RRID:AB_2636859
DAPI	Cat# C1002, Beyotime
MiRNA mimic	Cat# B02003, GenePharma
MiRNA inhibitor	Cat# B03001, GenePharma
Gene overexpression plasmid	Cat# C05001, GenePharma
MiRNA antagomir	Cat# B05001, GenePharma

Table 4. Statistical summary and analysis methods.

Figure reported	N	Normal distribution	Statistic	Statistic value (df)	p value	Variance source	Post hoc test	Post hoc p
1A, PD vs Control	5	Yes	Unpaired t test	t(8)=2.644	0.0295	Difference		
1B, PD vs Control	5	Yes	Unpaired t test	t(8)=3.418	0.0091	Difference		
1C, PD vs Control	5	Yes	Unpaired t test	t(8)=2.449	0.0400	Difference		
2A	3	Yes	one-way ANOVA	F（3,8）=41.01	<0.0001	Treatment		
2A, PBS vs LPS	3	Yes					Tukey	0.0025
2A, LPS+inhibitor NC vs LPS+ miR-132-3p inhibitor	3	Yes					Tukey	<0.0001
2B-TNF-α	3	Yes	one-way ANOVA	F（3,8）=62.48	<0.0001	Treatment		
2B-TNF-α，PBS vs LPS	3	Yes					Tukey	<0.0001
2B-TNF-α，LPS+ inhibitor NC vs LPS +miR-132-3p inhibitor	3	Yes					Tukey	0.001
2B-IL-1β	3	Yes	one-way ANOVA	F（3,8）=68.03	<0.0001	Treatment		
2B-IL-1β，PBS vs LPS	3	Yes					Tukey	<0.0001
2B-IL-1β，LPS+ inhibitor NC vs LPS +miR-132-3p inhibitor	3	Yes					Tukey	0.001
2B-IL-6	3	Yes	one-way ANOVA	F（3,8）=55.19	<0.0001	Treatment		
2B-IL-6，PBS vs LPS	3	Yes					Tukey	<0.0001
2B-IL-6，LPS+ inhibitor NC vs LPS +miR-132-3p inhibitor	3	Yes					Tukey	0.005
2C-TNF-α	3	Yes	one-way ANOVA	F（3,8）=38.98	<0.0001	Treatment		
2C-TNF-α，PBS vs LPS	3	Yes					Tukey	<0.0001
2C-TNF-α，LPS+ inhibitor NC vs LPS +miR-132-3p inhibitor	3	Yes					Tukey	0.0059
2C-IL-1β	3	Yes	one-way ANOVA	F（3,8）=70.75	<0.0001	Treatment		
2C-IL-1β，PBS vs LPS	3	Yes					Tukey	<0.0001
2C-IL-1β，LPS+ inhibitor NC vs LPS +miR-132-3p inhibitor	3	Yes					Tukey	0.001
2C-IL-6	3	Yes	one-way ANOVA	F（3,8）=86.8	<0.0001	Treatment		
2C-IL-6，PBS vs LPS	3	Yes					Tukey	<0.0001
2C-IL-6，LPS+ inhibitor NC vs LPS +miR-132-3p inhibitor	3	Yes					Tukey	0.001
3A	3	Yes	one-way ANOVA	F（2,6）=343.2	<0.0001	Treatment		
3A, mimic NC vs miR-132-3p mimic	3	Yes					Tukey	<0.0001

3B-TNF-α	3	Yes	one-way ANOVA	F(2,6)=47.96	0.0002	Treatment		
3B-TNF-α, mimic NC vs miR-132-3p mimic	3	Yes					Tukey	0.0003
3B-IL-1β	3	Yes	one-way ANOVA	F(2,6)=51.95	0.0002	Treatment		
3B-IL-1β, mimic NC vs miR-132-3p mimic	3	Yes					Tukey	0.0003
3B-IL-6	3	Yes	one-way ANOVA	F（2,6）=35	0.0005	Treatment		
3B-IL-6, mimic NC vs miR-132-3p mimic	3	Yes					Tukey	0.0016
3C-TNF-α	3	Yes	one-way ANOVA	F(2,6)=69.99	<0.0001	Treatment		
3C-TNF-α, mimic NC vs miR-132-3p mimic	3	Yes					Tukey	0.0002
3C-IL-1β	3	Yes	one-way ANOVA	F(2,6)=188.5	<0.0001	Treatment		
3C-IL-1β, mimic NC vs miR-132-3p mimic	3	Yes					Tukey	<0.0001
3C-IL-6	3	Yes	one-way ANOVA	F(2,6)=152.1	<0.0001	Treatment		
3C-IL-6, mimic NC vs miR-132-3p mimic	3	Yes					Tukey	<0.0001
4A	3	Yes	one-way ANOVA	F(3,8)=68.62	<0.0001	Treatment		
4A, PBS vs LPS	3	Yes					Tukey	<0.0001
4A, LPS+inhibitor NC vs LPS+ miR-132-3p inhibitor	3	Yes					Tukey	0.0050
4B	3	Yes	one-way ANOVA	F(3,8)=114.1	<0.0001	Treatment		
4B, PBS vs LPS	3	Yes					Tukey	<0.0001
4B, LPS+inhibitor NC vs LPS+ miR-132-3p inhibitor	3	Yes					Tukey	<0.0001
4C	3	Yes	one-way ANOVA	F（2,6）=9.25	0.0147	Treatment		
4C, mimic NC vs miR-132-3p mimic	3	Yes					Tukey	0.0461
4D	3	Yes	one-way ANOVA	F(2,6)=17.59	0.0031	Treatment		
4D, mimic NC vs miR-132-3p mimic	3	Yes					Tukey	0.0040
5A	3	Yes	one-way ANOVA	F(3,8)=35.92	<0.0001	Treatment		
5A, inhibitor NC vs miR-132-3p inhibitor	3	Yes					Tukey	0.006
5A, mimic NC vs miR-132-3p mimic	3	Yes					Tukey	0.0089
5B	3	Yes	one-way ANOVA	F(3,8)=13.63	0.0005	Treatment		
5B, inhibitor NC vs miR-132-3p inhibitor	3	Yes					Tukey	0.01
5B, mimic NC vs miR-132-3p mimic	3	Yes					Tukey	0.0382
5C-miR-132-3p	3	Yes	one-way ANOVA	F(3,8)=115.1	<0.0001	Treatment		
5C-miR-132-3p, IgG vs Ago2	3	Yes					Tukey	<0.0001

5C-GLRX	3	Yes	one-way ANOVA	F(3,8)=126.1	<0.0001	Treatment		
5C-GLRX, IgG vs Ago2	3	Yes					Tukey	<0.0001
5D, PBS vs LPS	3	Yes	two-way ANOVA	F(2,12)=12.1	0.0013	Interaction		
5D, PBS vs LPS	3	Yes	two-way ANOVA	F（2,12）=168.8	<0.0001	Main effect		
5F	3	Yes	one-way ANOVA	F(3,8)=9.623	0.0050	Treatment		
5F，wt-GLRX+ mimic NC vs wt-GLRX+miR-132-3p mimic	3	Yes					Tukey	0.0044
6A	3	Yes	one-way ANOVA	F(2,6)=75.16	<0.0001	Treatment		
6A, mimic NC vs miR-132-3p mimic	3	Yes					Tukey	0.002
6A, miR-132-3p mimic vs miR-132-3p mimic+GLRX	3	Yes					Tukey	<0.0001
6B	3	Yes	one-way ANOVA	F(2,6)=36.68	0.0004	Treatment		
6B, mimic NC vs miR-132-3p mimic	3	Yes					Tukey	0.0165
6B, miR-132-3p mimic vs miR-132-3p mimic+GLRX	3	Yes					Tukey	0.004
6C-TNF-α	3	Yes	one-way ANOVA	F（2,6）=43.7	0.0003	Treatment		
6C-TNF-α, mimic NC vs miR-132-3p mimic	3	Yes					Tukey	0.0003
6C-TNF-α, miR-132-3p mimic vs miR-132-3p mimic+GLRX	3	Yes					Tukey	0.001
6C-IL-1β	3	Yes	one-way ANOVA	F(2,6)=38.76	0.0004	Treatment		
6C-IL-1β, mimic NC vs miR-132-3p mimic	3	Yes					Tukey	0.0004
6C-IL-1β, miR-132-3p mimic vs miR-132-3p mimic+GLRX	3	Yes					Tukey	0.002
6C-IL-6	3	Yes	one-way ANOVA	F(2,6)=36.31	0.0004	Treatment		
6C-IL-6, mimic NC vs miR-132-3p mimic	3	Yes					Tukey	0.0013
6C-IL-6, miR-132-3p mimic vs miR-132-3p mimic+GLRX	3	Yes					Tukey	0.0005
6D-TNF-α	3	Yes	one-way ANOVA	F(2,6)=49.81	0.0002	Treatment		
6D-TNF-α, mimic NC vs miR-132-3p mimic	3	Yes					Tukey	0.0002
6D-TNF-α, miR-132-3p mimic vs miR-132-3p mimic+GLRX	3	Yes					Tukey	0.0011
6D-IL-1β	3	Yes	one-way ANOVA	F(2,6)=131.6	<0.0001	Treatment		
6D-IL-1β, mimic NC vs miR-132-3p mimic	3	Yes					Tukey	<0.0001
6D-IL-1β, miR-132-3p mimic vs miR-132-3p mimic+GLRX	3	Yes					Tukey	<0.0001
6D-IL-6	3	Yes	one-way ANOVA	F(2,6)=65.52	<0.0001	Treatment		
6D-IL-6, mimic NC vs miR-132-3p mimic	3	Yes					Tukey	0.0001

6D-IL-6, miR-132-3p mimic vs miR-132-3p mimic+GLRX	3	Yes					Tukey	0.003
6E	3	Yes	one-way ANOVA	F(2,6)=8.975	0.0157	Treatment		
6E, mimic NC vs miR-132-3p mimic	3	Yes					Tukey	0.0199
6E, miR-132-3p mimic vs miR-132-3p mimic+GLRX	3	Yes					Tukey	0.0312
6F	3	Yes	one-way ANOVA	F(2,6)=15.91	0.004	Treatment		
6F, mimic NC vs miR-132-3p mimic	3	Yes					Tukey	0.0047
6F, miR-132-3p mimic vs miR-132-3p mimic+GLRX	3	Yes					Tukey	0.0103
7A	6	Yes	one-way ANOVA	F（3,20）=65.02	<0.0001	Treatment		
7A, Saline vs MPTP	6	Yes					Tukey	<0.0001
7A, MPTP+ antagomir NC vs MPTP+miR-132-3p antagomir	6	Yes					Tukey	0.001
7B	6	Yes	one-way ANOVA	F（3,20）=35.37	<0.0001	Treatment		
7B, Saline vs MPTP	6	Yes					Tukey	<0.0001
7B, MPTP+ antagomir NC vs MPTP+miR-132-3p antagomir	6	Yes					Tukey	0.001